

Journal Pre-proof

New lipophenols prevent carbonyl and oxidative stresses involved in macular degeneration

Espérance Moine, Manel Boukhallat, David Cia, Nathalie Jacquemot, Laurent Guillou, Thierry Durand, Joseph Vercauteren, Philippe Brabet, Céline Crauste



PII: S0891-5849(20)31590-2

DOI: <https://doi.org/10.1016/j.freeradbiomed.2020.10.316>

Reference: FRB 14896

To appear in: *Free Radical Biology and Medicine*

Received Date: 24 September 2020

Revised Date: 22 October 2020

Accepted Date: 23 October 2020

Please cite this article as: E. Moine, M. Boukhallat, D. Cia, N. Jacquemot, L. Guillou, T. Durand, J. Vercauteren, P. Brabet, C. Crauste, New lipophenols prevent carbonyl and oxidative stresses involved in macular degeneration, *Free Radical Biology and Medicine*, <https://doi.org/10.1016/j.freeradbiomed.2020.10.316>.

This is a PDF file of an article that has undergone enhancements after acceptance, such as the addition of a cover page and metadata, and formatting for readability, but it is not yet the definitive version of record. This version will undergo additional copyediting, typesetting and review before it is published in its final form, but we are providing this version to give early visibility of the article. Please note that, during the production process, errors may be discovered which could affect the content, and all legal disclaimers that apply to the journal pertain.

© 2020 Elsevier Inc. All rights reserved.

1 New lipophenols prevent carbonyl and oxidative
2 stresses involved in macular degeneration.

3 *Espérance Moine*^{a,*}, *Manel Boukhallat*^a, *David Cia*^c, *Nathalie Jacquemot*^c, *Laurent Guillou*^b,
4 *Thierry Durand*^a, *Joseph Vercauteren*^a, *Philippe Brabet*^b and *Céline Crauste*^{a,*}.

5 ^a Institut des Biomolécules Max Mousseron (IBMM), Université de Montpellier, CNRS,
6 ENSCM, Montpellier, 34093, France

7 ^b Institut des Neurosciences de Montpellier, INSERM U1051, Université de Montpellier,
8 Montpellier, 34091, France

9 ^c Laboratoire de Biophysique Neurosensorielle, UMR INSERM 1107, Facultés
10 de Médecine et de Pharmacie, Clermont-Ferrand, 63000, France

11
12 * Correspondence: celine.crauste@umontpellier.fr; Tel.: +33-4-11-75-95-66,

13 esperance.moine@umontpellier.fr; Tel.: +33-4-11-75-95-66

14 **Keywords**

15 Lipophenol, PUFA, carbonyl stress, antioxidant, macular degeneration, structure-activity
16 relationship.

17

18 **Abbreviations**

19 A2E, *N*-retinylidene-*N*-retinylethanolamine; ABCA4, ATP binding cassette subfamily A
20 member 4; AGEs, advanced glycation end products; AMD, age-related macular degeneration;

21 ARPE-19, adult retinal pigment epithelial cell line-19; ASAP, atmospheric solids analysis probe;
22 *a*RAL, all-*trans*-retinal; BRB, blood retina barrier; BSMR, based on starting material recovery;
23 COS, carbonyl and oxidative stresses; DCC, dicyclohexylcarbodiimide; DCFDA, 2',7'-
24 dichlorofluorescein diacetate; DCM, dichloromethane; DHA, docosahexaenoic acid; DMAP,
25 dimethylaminopyridine; DMEM/F12, Dulbecco's Modified Eagle's Medium (DMEM)/Ham
26 F12; DMF, dimethylformamide; DMSO, dimethylsulfoxide; DNA, deoxyribonucleic acid; EC₅₀,
27 efficiency concentration 50; EGCG, epigallocatechin-3-*O*-gallate; EPA, eicosapentaenoic acid;
28 ESI, electrospray ionization; FBS, fetal bovine serum; 4-HHE, 4-hydroxyhexenal; 4-HNE, 4-
29 hydroxynonenal; HRMS, high resolution mass spectroscopy; LA, linoleic acid; Mp, melting
30 point; MTT, 3-(4,5-dimethylthiazol-2-yl)-2,5-diphenyl tetrazolium bromide; NMR, nuclear
31 magnetic resonance; Nrf2/Keap1, Nuclear factor (erythroid-derived 2)-like 2/Kelch-like ECH-
32 associated protein 1; PUFA, poly-unsaturated fatty acid; RCS, reactive carbonyl species; *R*_f,
33 retardation factor; ROS, reactive oxygen species; RPE, retinal pigment epithelium; TFA,
34 trifluoroacetic acid; THF, tetrahydrofuran; TIPS, triisopropylsilyl; TLC, thin layer
35 chromatography; UPLC, ultra-performance liquid chromatography; VEGF, vascular endothelial
36 growth factor.

37

38 **Abstract**

39 Dry age-related macular degeneration and Stargardt disease undergo a known toxic
40 mechanism caused by carbonyl and oxidative stresses (COS). This is responsible for
41 accumulation in the retinal pigment epithelium (RPE) of A2E, a main toxic pyridinium *bis*-
42 retinoid lipofuscin component. Previous studies have shown that carbonyl stress in retinal cells
43 could be reduced by an alkyl-phloroglucinol-DHA conjugate (lipophenol). Here, we performed a

44 rational design of different families of lipophenols to conserve anti-carbonyl stress activities and
45 improve antioxidant properties. Five synthetic pathways leading to alkyl-(poly)phenol
46 derivatives, with phloroglucinol, resveratrol, catechin and quercetin as the main backbone, linked
47 to poly-unsaturated fatty acid, are presented. These lipophenols were evaluated in ARPE-19 cell
48 line for their anti-COS properties and a structure-activity relationship study is proposed.
49 Protection of ARPE-19 cells against A2E toxicity was assessed for the four best candidates.
50 Finally, interesting anti-COS properties of the most promising quercetin lipophenol were
51 confirmed in primary RPE cells.

52

53 **Introduction**

54 Oxidative stress, resulting from an overproduction of reactive oxygen species (ROS) within
55 cells or in the extracellular matrix, highly damages key cellular proteins, lipids and DNA.
56 Reactive carbonyl species (RCS), such as sugars and osones, endogenous aldehydes or
57 metabolites derived from lipid oxidation, are involved in glycation and cross-linking reactions
58 and thus, affect cellular viability leading to tissue injury. These two carbonyl and oxidative stress
59 (COS) mechanisms play a crucial role in aging-associated pathologies, like age-related macular
60 degeneration (AMD), or in some inherited forms of macular degeneration, such as Stargardt
61 disease [1–3]. AMD is one of the primary causes of central and irreversible visual loss among
62 the elderly in occidental countries, and there is no treatment currently available to stop retinal
63 degeneration, especially in the prevalent dry form (80-85% of cases). COS mechanisms are
64 responsible for the accumulation in retinal pigment epithelium (RPE) of a toxic *bis*-retinoid
65 conjugate called A2E (its photoisomers and its oxidized metabolites). Pathologic A2E
66 biosynthesis occurs when all-*trans*-retinal (*at*RAL), rather than undergoing reduction to retinol in

67 the RPE, accumulates abnormally in photoreceptors. This accumulation can be due to age
68 (AMD) or loss of function of the ABCA4 transporter (Stargardt disease) [2]. Two molecules of
69 this reactive aldehyde (RCS) in excess, condense with one molecule of phosphatidyl
70 ethanolamine (carbonyl stress step) into an unstable dihydropyridinium *bis*-retinoid.
71 Transformation of the dihydropyridinium *bis*-retinoid into A2E then arises during the oxidative
72 step leading to a more stable pyridinium form. A2E and its various oxidative metabolites are the
73 major constituent of lipofuscin, a marker of AMD. The massive accumulation of lipofuscin in the
74 RPE (following phagocytosis of photoreceptor outer segments) is cytotoxic and causes
75 progressive RPE cell death and subsequent photoreceptor degeneration [4]. A2E cytotoxicity is
76 explained by several mechanisms: loss of membrane integrity due to its amphiphilic properties
77 during membrane integration; increase of oxidative stress by the generation of singlet oxygen
78 during exposition to blue light; metabolization in A2E-oxidized metabolites resulting in DNA
79 lesions [5–7]. Limitation of A2E biosynthesis (by clearance of *ar*RAL) and oxidation is therefore
80 an attractive target to slow the progression of macular degeneration [8].

81 Based on epidemiology studies, natural plant antioxidants, such as (poly)phenols, secondary
82 metabolites that protect plants from several aggressions, are efficient at protecting animal
83 organisms against oxidative stress. Some (poly)phenol structures have been reported to protect a
84 variety of retinal cell types from oxidative stress-induced cell death [9–11]. Such activity may be
85 related to their capacity to scavenge directly excess ROS, or to stimulate the enzymatic
86 antioxidant defenses of the organism through Nrf2/Keap1 signaling pathway[12,13]. Moreover,
87 recent literature addressed the efficiency of (poly)phenols to inhibit Advanced Glycation End
88 product formation (AGEs), which result from both carbonyl and oxidative stresses [14,15], and
89 to act also as anti-carbonyl stress derivatives by trapping toxic RCS (glyoxal, acrolein, 4-

90 hydroxynonenal (4-HNE)) [16–18].

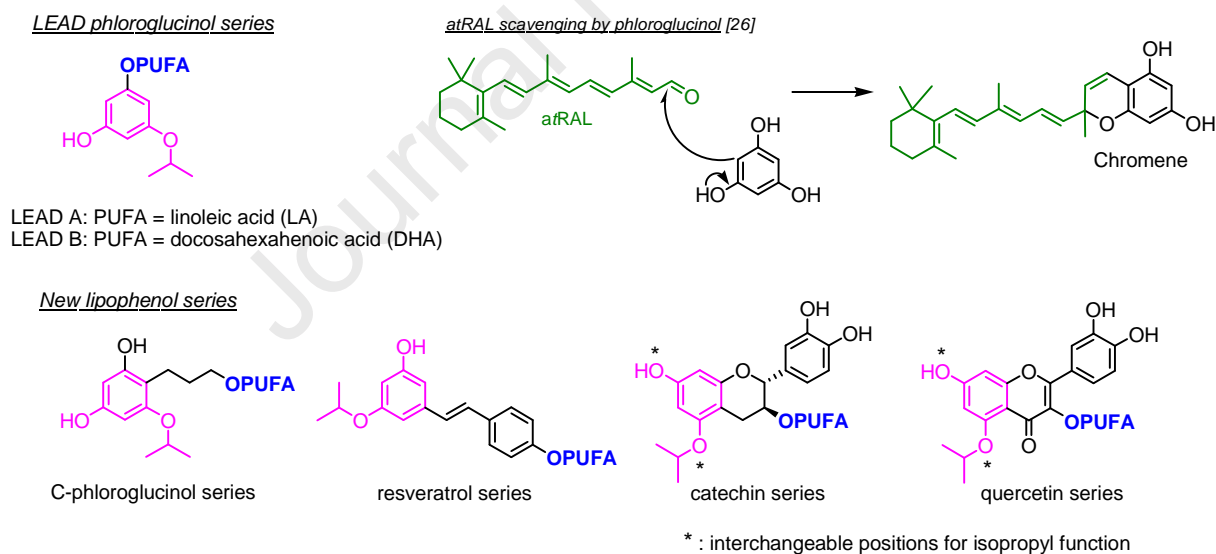
91 Unfortunately, while showing interesting *in vitro* protection, the limited bioavailability of most
92 (poly)phenols (weak drug absorption, high systemic metabolization, restricted cell
93 penetration...) negatively influences their *in vivo* potency and thus their development as drug
94 candidates. Increasing the lipophilicity of those (poly)phenols may be a useful way to improve i)
95 their protective effect on lipid membranes or lipid derivatives (such as A2E), ii) their absorption
96 [19], and iii) their formulation for *in vivo* administration [20–22]. In our previous work, we
97 synthesized lipophenols (or phenolipids), polyunsaturated fatty acid (PUFA) linked to alkyl-
98 phloroglucinol (LEAD A/B, **Figure 1**), that were designed to reduce carbonyl stress associated
99 with retinal dystrophies [23,24]. The main objective of those lipophenols was to avoid/slow the
100 pace of A2E formation by scavenging *α*RAL (**Figure 1**). To increase lipophilicity and cellular
101 permeability of starting (poly)phenol, PUFAs were preferred to saturated ones, due to their
102 observed benefits in an AMD clinical trial [25]. Both isopropyl-phloroglucinols linked to linoleic
103 acid (C18:2 n-6; LA - LEAD A, **Figure 1**) and docosahexaenoic acid (C22:6 n-3; DHA - LEAD
104 B, **Figure 1**) showed promising protection of RPE cells against *α*RAL toxicity. A isopropyl
105 functional group was rationally selected to increase the nucleophilic properties of the aromatic
106 cycle involved in the trapping of aldehyde function of *α*RAL and leading to the formation of a
107 stable non-toxic chromene adduct (**Figure 1**) [23,26]. Both isopropyl and PUFA parts were
108 proven to be indispensable in a phloroglucinol series (LEAD A and LEAD B) to ensure cell
109 protection against carbonyl stress in cellular assays [23,24]. The DHA analogue (LEAD B) was
110 selected for further *in vivo* evaluations due to several benefits of this omega-3 lipid: i) the high
111 proportion of DHA in the membrane of photoreceptor outer segments, ii) its ability to reach the
112 retina through PUFA transports [27]; iii) recent data showing that dietary supplementation with

113 high doses of DHA/EPA significantly improves the visual acuity of AMD patients [25]; and iv)
114 the report that specific oxidative metabolites of DHA (Neuroprotectin D1) protect RPE cells
115 against oxidative stress [28]. Intravenous administration of LEAD B allowed photoreceptor
116 protection against acute light-induced degeneration in a mouse model used for the development
117 of novel therapeutics for Stargardt disease (*Abca4*^{-/-} mice) [29,30]. Despite interesting
118 preliminary *in vivo* protection observed using LEAD B, this phloroglucinol derivative lacks
119 efficiency to reduce ROS production and cellular oxidative stress. In the present study, we report
120 new potent alkyl-lipophenols that act on both carbonyl and oxidative stresses, to reduce *atRAL*
121 toxicity, and oxidation associated with A2E formation, metabolism and toxicity, critical steps
122 involved in photoreceptor degeneration.

123 Several possibilities have been proposed to increase antioxidant activities while preserving
124 anti-carbonyl stress properties. First, using the same (poly)phenol backbone, PUFA was linked
125 directly to the aromatic cycle to free one phenolic function of the phloroglucinol involved in the
126 antioxidant activity (C-phloroglucinol series, **Figure 1**). Second, new series of lipophenols were
127 also developed from natural (poly)phenols, different from phloroglucinol, meeting the criterion
128 that the starting (poly)phenol contained an isopropyl-resorcinol framework mimicking the
129 phloroglucinol backbone, as this was indispensable for the protection against carbonyl stress
130 [23,24]. More effective natural antioxidants, such as resveratrol stilbenoid (true vinylogous
131 analogue of phloroglucinol), or flavonoids, such as quercetin or catechin, all of which were
132 reported to trap aldehyde function in cell free assays [18,31,32] and to protect ARPE-19 cells
133 against A2E photo-oxidation damage [33–35], have been proposed as new anti-COS alkyl-
134 lipophenol series (**Figure 1**). Nine novel alkyl-lipophenol-PUFAs have been synthesized using
135 original chemical strategies. Toxicity assays, protection against a lethal concentration of *atRAL*

136 and reduction of H₂O₂ induced ROS production, were used to first screen these molecules in
 137 ARPE-19 cells. The necessity of the isopropyl and the PUFA parts for carbonyl stress protection
 138 has been highlighted with all new (poly)phenol backbones (resveratrol, catechin and quercetin).
 139 The ability to preserve antioxidant properties, despite reduction of free phenolic functions
 140 compared to native (poly)phenols, has been studied. Best DHA-lipophenol conjugates offering
 141 both oxidative and carbonyl stress protection, were compared with LEAD B, for their ability to
 142 reduce A2E toxicity during photo-oxidation process in RPE. According to the comparison of
 143 both carbonyl and oxidative stress protection, a new alkyl-quercetin-PUFA conjugate has been
 144 highlighted. Cell protection was finally validated with this lipophenol in primary RPE cells, as
 145 primary cultures are likely to reflect *in vivo* cell morphology and function more accurately.

146



147

148

Figure 1. Chemical structures of developed lipophenol series.

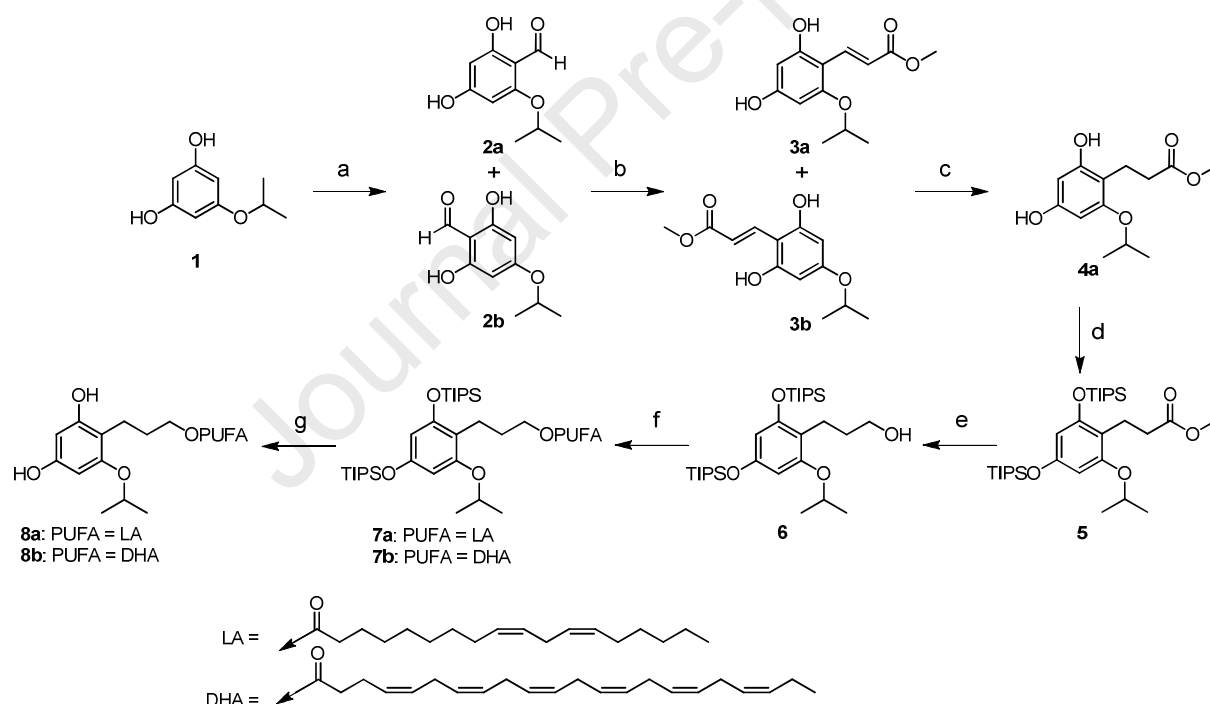
149

150 Results and Discussion

151 1. Synthesis and anti-COS evaluation of C-phloroglucinol derivatives

152 The first chemical changes considered to increase antioxidant capacity concerned the link of
 153 the PUFA moiety. Indeed, releasing one more phenolic function on the phloroglucinol (P)
 154 backbone should allow better ROS scavenging properties. This modification was investigated
 155 through a C-alkylation on the phloroglucinol aromatic ring, by the introduction of a
 156 hydroxylated-alkyl spacer, in order to perform PUFA functionalization. The synthesis of the two
 157 C-linker analogues (**8a/b**) of LEAD A (P-OiP-OLA) and LEAD B (P-OiP-ODHA) is described
 158 in **Scheme 1**.

159

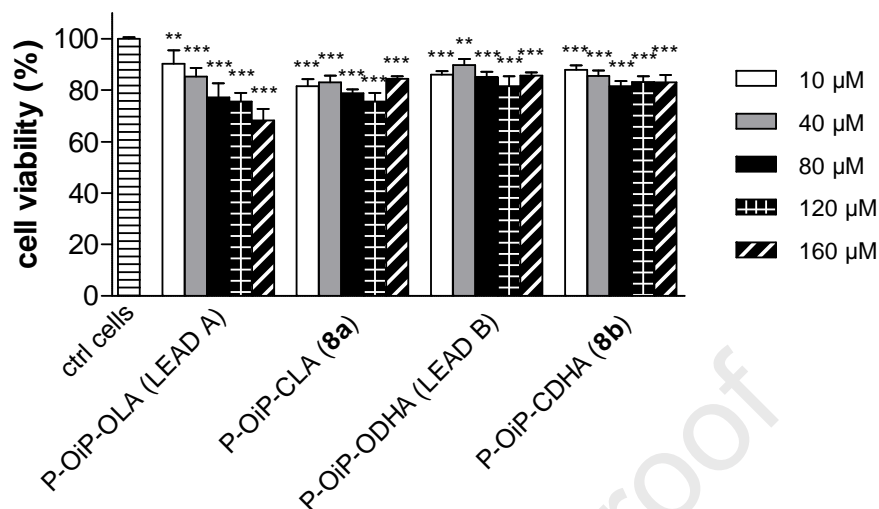
160 **Scheme 1. Chemical pathway leading to C-phloroglucinol derivatives^a**

167

168 Starting from mono-isopropyl phloroglucinol **1** [23], a Gattermann-Koch formylation [36] lead
169 to salicylic aldehydes **2a/2b** (80/20) in 64% combined yield. The next Wittig reaction was
170 performed on the mixture of **2a/2b** for a two-carbon homologation, and the resulting two α,β -
171 unsaturated esters **3a/3b** were reduced under hydrogen in the presence of Pd/C catalyst which
172 after purification lead to the isolation of isomer **4a**. Phenolic functions were then protected by
173 silylated protecting groups (compound **5**). The alcohol **6** was obtained after the ester reduction
174 and was coupled either with LA or DHA using classical Steglich coupling conditions. Finally,
175 LA and DHA desired conjugates (respectively **8a** and **8b**) were obtained after deprotection of
176 silylated phenolic function in the presence of $\text{NEt}_3/3\text{HF}$.

177 *In vitro* evaluations of the C-phloroglucinol derivatives were performed on the ARPE-19 cell
178 line. All compounds were tested at various concentrations in the range of 0-160 μM for
179 cytotoxicity assessment, and in the range of 0-80 μM for anti-COS evaluation. Regarding the
180 new C-phloroglucinol derivatives (**8a** and **8b**), our main concerns were to maintain anti-carbonyl
181 stress activity, despite the reduction of one nucleophilic C-alkylation site (on the aromatic cycle)
182 compared to LEAD A/B structures, and to increase antioxidant properties by releasing a phenolic
183 function. As shown in **Figure 2**, there is no apparent cytotoxicity due to the modification of the
184 lipid position.

185



186

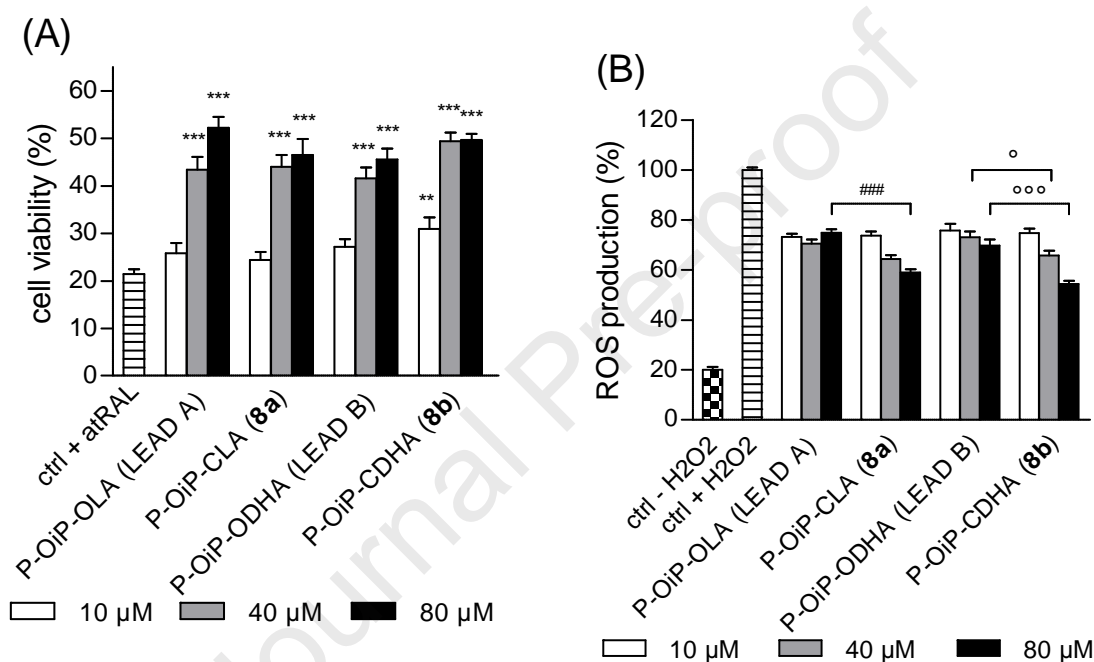
187 **Figure 2.** Evaluation of cytotoxicity of C-phloroglucinol derivatives; P-OiP-OLA (LEAD A)
 188 [24], P-OiP-CLA (**8a**), P-OiP-ODHA (LEAD B) [23] and P-OiP-CDHA (**8b**). Results are
 189 expressed in mean \pm SEM and are from $n = 3-5$ independent experiments. ARPE-19 cell viability
 190 (MTT) after incubation of phloroglucinol derivatives (0-160 μM). The data are expressed as the
 191 percentage of non-treated control cells. * $p < 0.05$, ** $p < 0.01$, *** $p < 0.001$, versus non-
 192 treated control cells.

193

194 Anti-carbonyl stress activity of C-phloroglucinol derivatives is evaluated by comparing cell
 195 survival in presence of a toxic concentration of carbonyl stressor *atRAL*, and is represented in
 196 **Figure 3A**. The two new C-phloroglucinol derivatives (**8a** and **8b**) displayed interesting
 197 protective properties, increasing cell viability (at 80 μM) of + 25% for LA derivative (**8a**) and +
 198 28% for DHA derivative (**8b**), compared to non-treated and *atRAL*-exposed cells. No statistical
 199 differences in cell protection were observed under these conditions between P-OiP-OLA (LEAD
 200 A) versus P-OiP-CLA (**8a**) and between P-OiP-ODHA (LEAD B) versus P-OiP-CDHA (**8b**), at
 201 equivalent concentrations. Modification of the PUFA position on the phloroglucinol backbone
 202 did not affect the anti-carbonyl stress activity of the derivative: the PUFA moiety can be
 203 introduced indifferently on a phenolic function or with a spacer on the aromatic core. This result

204 is in agreement with the literature, as phloretine, a natural phloroglucinol analogue with a
 205 substituent on the aromatic ring, is also able to trap toxic aldehydes, such as acrolein, a toxic
 206 aldehyde found in cigarette smoke and involved in AMD via induction of oxidative damage in
 207 RPE cells, or 4-HNE, derived from lipid peroxidation [31].

208



209 **Figure 3.** *In vitro* anti-COS evaluation of C-phloroglucinol derivatives. Comparison of P-OiP-
 210 OLA (LEAD A) [24], P-OiP-CLA (**8a**), P-OiP-ODHA (LEAD B) [23] and P-OiP-CDHA (**8b**)
 211 activities. Results are expressed in mean \pm SEM and are from $n = 3-5$ independent experiments.
 212 (A) Anti-carbonyl stress assay: ARPE-19 cell viability (MTT) after incubation of phloroglucinol
 213 derivatives (0-80 μ M) and atRAL (15 μ M). The data are expressed as the percentage of non-
 214 treated and non-exposed to atRAL control cells. * $p < 0.05$, ** $p < 0.01$, *** $p < 0.001$, versus
 215 non-treated and exposed to atRAL cells. (B) Antioxidant assay: representation of ROS
 216 production (DCFDA probe) after incubation of phloroglucinol derivatives (0-80 μ M) and H₂O₂
 217 (600 μ M) in ARPE-19 cells. The data are expressed as the percentage of non-treated and
 218 exposed to H₂O₂ cells. All conditions have a p -value < 0.001 versus non-treated and exposed to
 219 H₂O₂ control cells. # $p < 0.05$, ## $p < 0.01$, ### $p < 0.001$, versus P-OiP-OLA (LEAD A) at the
 220 same concentration. ° $p < 0.05$, °° $p < 0.01$, °°° $p < 0.001$, versus P-OiP-ODHA (LEAD B) at the
 221 same concentration.

222

223 The main objective of the synthesis of compounds **8a** and **8b** was to increase antioxidant
224 properties of the LEADs A and B in cell experiments. As expected, **8a** and **8b** logically showed
225 weaker antioxidant activity compared to phloroglucinol (data not shown). Compared to untreated
226 cells, C-phloroglucinol analogues were able to decrease H₂O₂ induced ROS production by 41%
227 for LA derivative (**8a**) and 46% for DHA derivative (**8b**) at 80 μM (**Figure 3B**). Thus, a
228 significant improvement in antioxidant activity was observed using C-phloroglucinols (**8a/8b**)
229 that show a dose-dependent effect compared to LEAD A and B. Direct hydroxyl radical
230 scavenging activity of phloroglucinol has been previously reported [26,37], and the liberation of
231 one phenolic function explains the increased antioxidant efficacy of C-phloroglucinol derivatives
232 (**8a** and **8b**) compared to LEAD A and LEAD B, that reduce ROS production by only 25% and
233 30% at 80 μM, respectively.

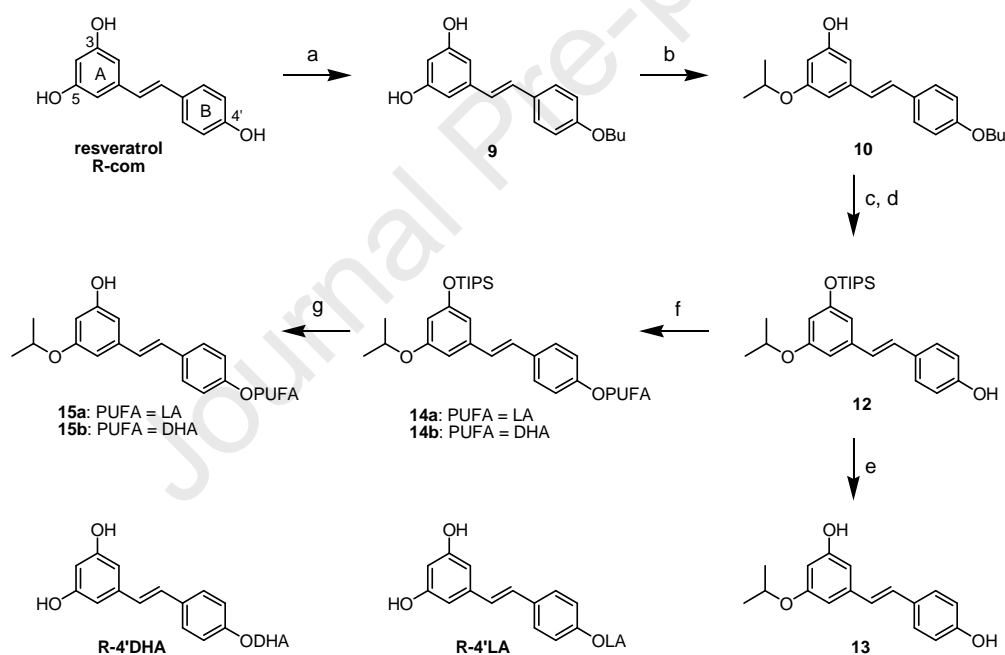
234

235 2. Synthesis and anti-COS evaluation of resveratrol lipophenol analogues

236 Resveratrol (R), a major active phytoalexin from the stilbene family (3,4',5'-
237 trihydroxystilbene), is mainly found in *Vitis vinifera* (Vitaceae) stalks and in the roots of
238 *Fallopia japonica var. japonica* (Polygonaceae). Resveratrol has a wide range of biological
239 activities including anti-bacterial and anti-fungal properties [38], antioxidant activity [10,39],
240 and anti-inflammatory properties [40]. Furthermore, previous evaluations on RPE cell assays
241 highlighted the benefit of resveratrol in reducing VEGF effect and increasing natural antioxidant
242 enzymatic and molecular defenses [40]. Resveratrol should not only be considered as a simple
243 ROS scavenger. The work of Vlachogianni et al. shows better radical scavenging activity of 4'-
244 acetylated resveratrol compared to 3-acetylated analogues [41]; we decided therefore to link the
245 PUFA at the 4' position of resveratrol. The isopropyl moiety was introduced at the 5 position in

246 order to keep the alkyl-resorcinol moiety, which was proven to be responsible for high anti-
 247 carbonyl stress activity on phloroglucinol series [23]. In order to confirm the necessity of alkyl as
 248 well as PUFA moieties on the resveratrol backbone, as we did previously with phloroglucinol
 249 [23,24], we produced in addition to alkyl resveratrol-PUFA (**15a/b**), an isopropyl-resveratrol
 250 derivative not linked to PUFA (**R-5OiP 13**, **Scheme 2**) and derivatives linked to PUFAs without
 251 alkyl function named resveratrol-4'LA (**R-4'LA**) and resveratrol-4'DHA (**R-4'DHA**), both
 252 synthesized as previously described [42,43].

253 Scheme 2. Synthesis and chemical structures of resveratrol derivatives^a



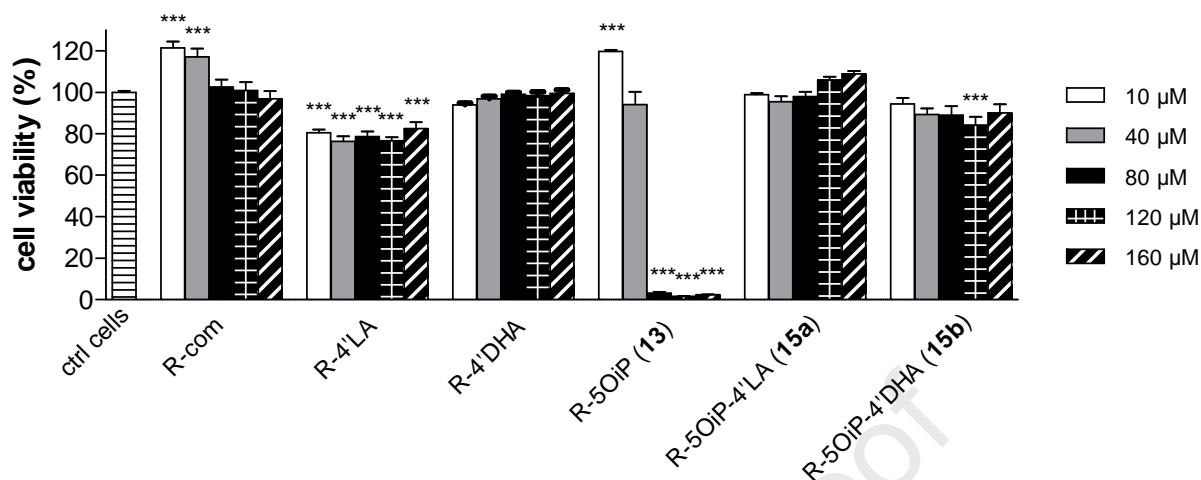
255 ^aReagents and conditions: (a) 2-methyl-butan-2-ol, vinyl butyrate, Novozyme 435 (CALB), 40
 256 °C, 8 days, 52%; (b) diisopropylsulfate, K₂CO₃, acetone, rt, 24 h, 22% (67% BSMR); (c) TIPS-
 257 OTf, DIPEA, THF, rt, 6 h, 63%; (d) NH₃/MeOH, DCM, 0 to 5 °C, 24 h, 80%; (e) NEt₃/3HF,
 258 THF, rt, 23 h, 67%; (f) PUFA, DCC, DMAP, DCM, rt, **14a**: 35 min, 83% and **14b**: 2 h, 46%; (g)
 259 NEt₃/3HF, THF, rt, **15a**: 19 h, 67% and **15b**: 20 h, 64%.

260

261 A tedious step to access the desired alkylated resveratrols **15a/b**, was the isopropylation of the
262 5 position of resveratrol as the 4' position is the more reactive. Utilization of the supported lipase
263 Novozyme 435 (Immobilized lipase from *Candida antarctica*) was efficient and selective to
264 protect the 4' position of resveratrol, using vinyl butyrate (52%). Alkylated compound **10** was
265 then obtained using diisopropylsulfate and K_2CO_3 at room temperature for 24 h [44]. Successive
266 protection of the resulting phenol with TIPS groups, and deprotection of the butyrate in position
267 4' using ammonia solution in MeOH, gave access to compound **12**, which could be esterified by
268 LA or DHA through classical Steglich conditions, or desilylated to give the desired isopropylated
269 resveratrol (R-5OiP, **13**). Final desilylation of the esterified compounds (**14a** and **14b**) gave
270 access to the desired LA- and DHA-isopropylated resveratrol derivatives **15a** and **15b** using mild
271 $NEt_3/3HF$ reagent.

272 First, cytotoxicity of resveratrol derivatives on ARPE-19 cell line was evaluated and is
273 represented in **Figure 4**. No dose dependent toxicity was observed for LA or DHA alkyl-
274 resveratrol **15a/b** up to 160 μM . Introduction of only the isopropyl moiety on resveratrol (R-
275 5OiP, compound **13**), led to highly toxic effects from 80 μM . Interestingly, association of LA or
276 DHA and isopropyl moieties (compounds **15a** and **15b**) resulted in absent or weak toxicity up to
277 160 μM , suggesting a stability of the lipophenol ester during the toxicity assay. Indeed, if the
278 ester link was easily cleaved, the release of the remaining R-5OiP (**13**) would have induced high
279 toxicity levels.

280



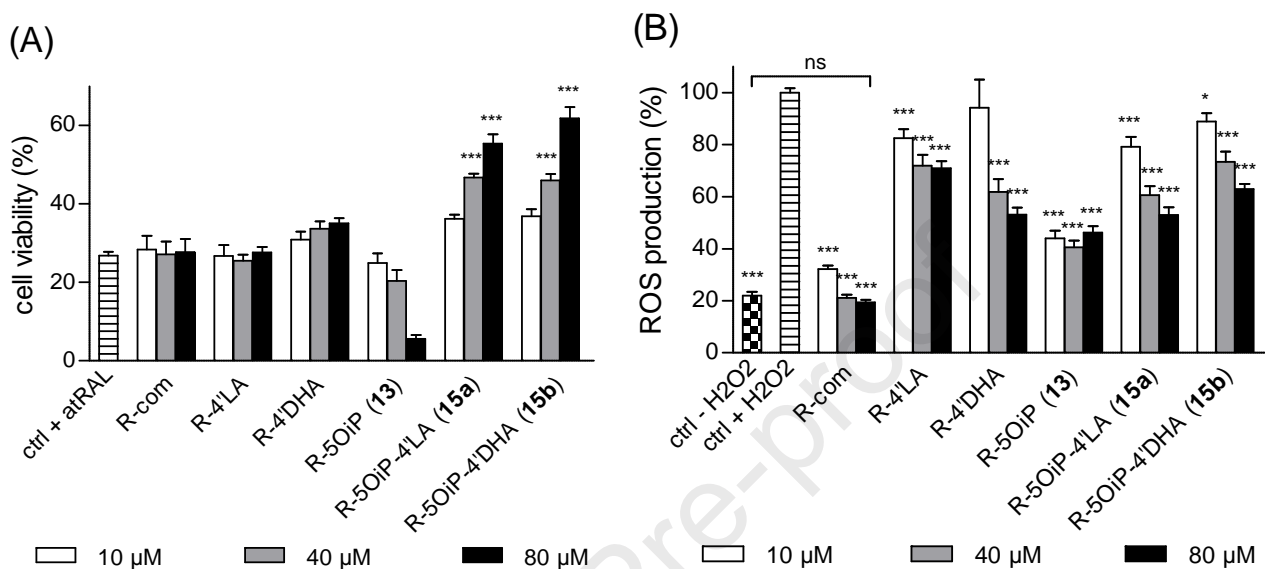
281
282

283 **Figure 4.** Evaluation of cytotoxicity of resveratrol derivatives; natural resveratrol (R-com), R-
284 4'LA [42], R-4'DHA [43], R-5OiP (**13**), R-5OiP-4'LA (**15a**) and R-5OiP-4'DHA (**15b**). Results
285 are expressed in mean \pm SEM and are from $n = 3-5$ independent experiments. ARPE-19 cell
286 viability (MTT) after incubation of resveratrol derivatives (0-160 μ M). The data are expressed as
287 the percentage of non-treated control cells. * $p < 0.05$, ** $p < 0.01$, *** $p < 0.001$, versus non-
288 treated control cells.

289

290 In order to study the impact of the isopropyl, as well as the PUFA moieties, for anti-carbonyl
291 stress activity, commercial resveratrol (R-com), R-5OiP (**13**), R-4'LA and R-4'DHA [42,43]
292 were evaluated and compared to the new alkyl lipophenols **15a** and **15b** (**Figure 5A**).
293 Derivatives bearing both alkyl and PUFA substituents, presented the best protective effects under
294 carbonyl stress: 29% and 35% increase in viability using 80 μ M of R-5OiP-4'LA (**15a**) and R-
295 5OiP-4'DHA (**15b**), respectively. By contrast, no significant cell protection was observed for the
296 four other derivatives (R-com, R-5OiP (**13**), R-4'LA and R-4'DHA), whose chemical structures
297 presented isopropyl, or PUFA substituent, or no additional substituent. These interesting results
298 confirm the importance of the *O*-isopropyl-resorcinol group, as well as the necessity of a PUFA
299 substituent for the anti-carbonyl stress activity, as was observed for the phloroglucinol LEAD
300 series [23]. In agreement with the toxicity results, the protective effect of the esterified

301 compounds (**15a** and **15b**) and the loss in cell viability observed using R-5OiP (**13**), confirm the
 302 stability of the ester bound of these lipophenols during the cell protection assay.



303 **Figure 5.** *In vitro* anti-COS evaluation of resveratrol derivatives. Comparison of natural
 304 resveratrol (R-com), R-4'LA [42], R-4'DHA [43], R-5OiP (**13**), R-5OiP-4'LA (**15a**) and R-
 305 5OiP-4'DHA (**15b**) activities. Results are expressed in mean \pm SEM and are from $n = 3-5$
 306 independent experiments. (A) Anti-carbonyl stress assay: ARPE-19 cell viability (MTT) after
 307 incubation of resveratrol derivatives (0-80 μM) and aRAL (15 μM). The data are expressed as
 308 the percentage of non-treated and non-exposed to aRAL control cells. * $p < 0.05$, ** $p < 0.01$,
 309 *** $p < 0.001$, versus non-treated and exposed to aRAL cells. (B) Antioxidant assay:
 310 representation of ROS production (DCFDA probe) after incubation of resveratrol derivatives (0-
 311 80 μM) and H₂O₂ (600 μM) in ARPE-19 cells. The data are expressed as the percentage of non-
 312 treated and exposed to H₂O₂ cells. * $p < 0.05$, ** $p < 0.01$, *** $p < 0.001$, versus non-treated and
 313 exposed to H₂O₂ cells.

314

315 The anti-carbonyl potential of resveratrol has been described by Wang et al. who demonstrated
 316 the formation of an adduct by co-incubation of resveratrol with acrolein at equimolar
 317 concentration [18], and by Shen et al. with methyl glyoxal [45]. Resveratrol was able to scavenge
 318 toxic aldehydes and formed an heterocyclic ring at the C-2 and C-3 positions through
 319 nucleophilic addition. Resveratrol protection of acrolein-treated cells was also attributed to a

320 direct stimulatory action on mitochondrial bioenergetics [46]. Here, in our cellular assay, natural
321 resveratrol did not display sufficient anti-carbonyl stress activity to counteract toxic effects of
322 high doses of *at*RAL. However, increasing the nucleophilicity of resorcinol backbone with an
323 isopropyl group, and increasing lipophilicity of this polyphenol by addition of a PUFA,
324 prevented aldehyde toxicity.

325 Regarding the antioxidant profiles of resveratrol derivatives, shown in **Figure 5B**, 40 μ M
326 commercial resveratrol (R-com) was able to reach the oxidative status of cells that did not
327 received the oxidant stressor H_2O_2 . Logically, the introduction of a fatty acid moiety (LA or
328 DHA) and/or an alkyl residue masking the phenolic function, led to a loss of antioxidant capacity
329 compared to R-com. However, both the studied alkyl-lipophenols R-5OiP-4'LA (**15a**) and R-
330 5OiP-4'DHA (**15b**) were still potent antioxidant derivatives, as, at 80 μ M, they decreased ROS
331 production by up to 47% and 37%, respectively. The reduction of the accessibility of two
332 phenolic functions on the resveratrol backbone still allowed **15a** and **15b** to be potent
333 antioxidants able to reduce oxidative status in a dose-dependent manner.

334 Thus, both resveratrol alkyl-lipophenols **15a** and **15b** exhibited an interesting protection
335 against the double COS in ARPE-19 cells.

336

337 *3. Synthesis and anti-COS evaluation of flavonoid lipophenol analogues*

338 Flavonoids are widely known as potent antioxidants by direct or indirect action [13,47,48]. We
339 worked on two natural flavonoid derivatives, quercetin and catechin (**Figure 1**).

340 Quercetin (3,3',4',5,7-pentahydroxyflavone, Q) is a plant flavonol, which is present in various
341 quantities in many fruit and vegetables, including apple, cranberry, red onion, asparagus,
342 spinach, walnuts and coriander. Over the past decades, quercetin has gained research interest due

343 to its numerous pharmacological activities. In addition to its antioxidant properties, quercetin
344 was proven to have anti-inflammatory, antidiabetic, anticancer, cardiovascular, hepato-
345 protective, antiplatelet, antibacterial and neuroprotective properties [49]. Regarding its
346 antioxidant action, quercetin acts by scavenging free radicals, and also increases antioxidant
347 enzymes, such as glutathione peroxidase, superoxide dismutase and catalase [50]. (+)-Catechin
348 (C) is a flavanol abundant in berries, chocolate, cacao and green tea that makes a significant
349 contribution to total dietary antioxidant intake. Catechin is the monomer of proanthocyanidin B2,
350 whose protection against A2E photo-oxidation-induced apoptosis has been shown in ARPE-19
351 cells [35]. Compared to quercetin, catechin should have increased nucleophilic properties
352 coming from the A ring, due to the absence of the carbonyl function link to this aromatic cycle.

353 Distinctive chemical structures related with flavonoid antioxidant activities have been
354 established including hydroxyl groups of the A-ring (resorcinol), ortho-dihydroxy arrangement
355 in the B-ring (catechol), and in the case of quercetin, C2-C3 unsaturated bond combined with C-
356 4 carbonyl group in the C-ring [48]. Moreover, the position instead of total number of hydroxyl
357 groups, considerably influences the efficiency of antioxidant activity [51]. The B-ring hydroxyl
358 structure is the utmost significant actor of scavenging oxygen free radicals [52]. In addition,
359 according to the study of Hong et al. [53], radical scavenging properties of catechin seem to be
360 less affected by acylation at the 3 or 7 position compared to acylation of the catechol moiety.
361 Thereby, in order to conserve the best antioxidant properties, the B-ring, corresponding to the
362 catechol moiety, was left free of any substituent, and position 3 was selected to introduce the
363 PUFA moiety on both catechin and quercetin. Finally, to preserve the alkylated resorcinol group
364 needed for the anti-carbonyl stress activity in both phloroglucinol and resveratrol series, two
365 positions of the A-ring, that mimic the resorcinol moiety of the LEADs A/B, were selected to

366 introduce the isopropyl; both positions 5 and 7 were alkylated in order to evaluate the most
 367 favorable for carbonyl stress protection. As for resveratrol derivatives, lipophilic catechin and
 368 quercetin bearing only the PUFA moiety (C-3PUFA and Q-3PUFA) [42], and alkyl-flavonoids
 369 bearing only the isopropyl moiety (C-5OiP **18b**, C-7OiP **18a**, Q-5OiP **23** and Q-7OiP **35**), were
 370 produced to evaluate their impact on biological properties.

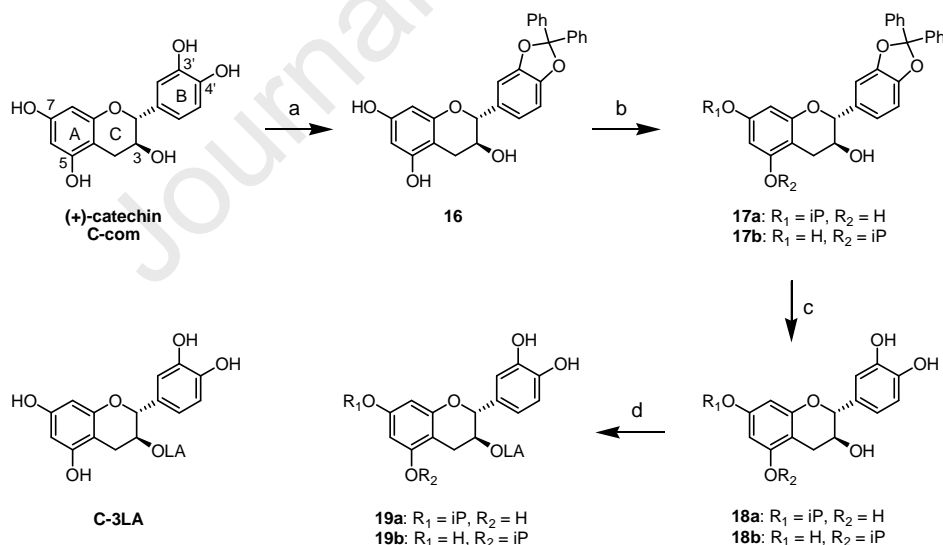
371

372 3.1. Catechin lipophenols synthesis and evaluation

373 Synthesis of alkyl-catechin derivatives C-7OiP (**18a**) and C-5OiP (**18b**), as well as the alkyl-
 374 lipophenol derivatives C-3LA-7OiP (**19a**) and C-3LA-5OiP (**19b**), are presented in **Scheme 3**.

375

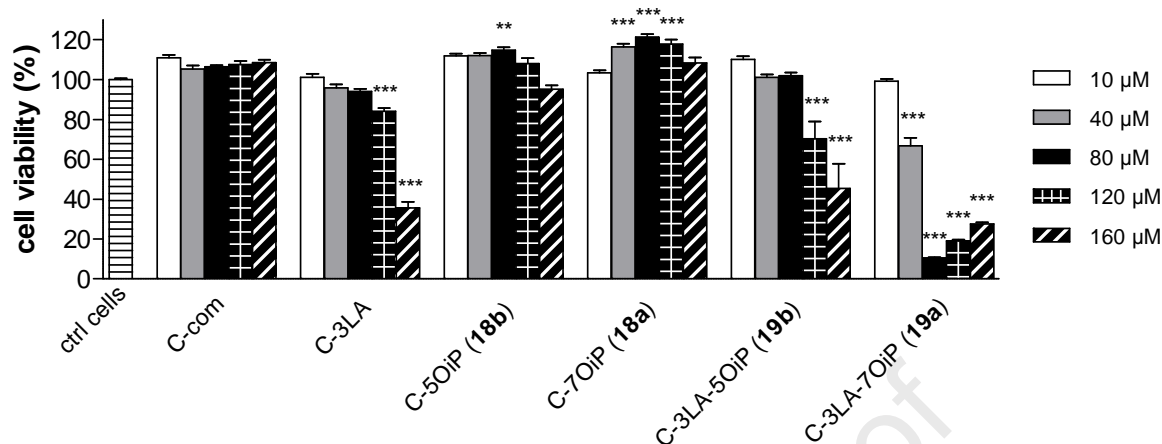
376 **Scheme 3. Synthesis and chemical structures of (+)-catechin derivatives^a**



383 The first step of the synthesis was the protection of the catechol moiety of catechin by a
384 diphenyldioxole in acetonitrile [54]. The alkylation step allowed access to both isomers **17a** and
385 **17b** with 1/1 proportion in 37% yield. The two isomers were separated by column
386 chromatography and engaged separately for the end of the synthesis. Deprotection of the
387 catechol was performed by hydrogenation using palladium hydroxide and led to the desired
388 alkylated catechin derivatives: C-7OiP (compound **18a**) and C-5OiP (compound **18b**). The
389 lipophenols were then obtained using TFA and freshly prepared linoleyl chloride, as described
390 by Uesato et al. [55]. Compounds C-3LA-7OiP (**19a**) and C-3LA-5OiP (**19b**) were isolated in
391 sufficient quantities to be evaluated *in vitro*.

392 Commercial catechin (C-com), as well as the two alkylated catechins C-5OiP (**18b**) and C-
393 7OiP (**18a**), displayed no toxicity on ARPE-19 cells up to 160 μ M (**Figure 6**). However, C-3LA
394 [42] and C-3LA-5OiP (**19b**) displayed an important cell death above 120 μ M. Toxicity was even
395 higher for C-3LA-7OiP (**19a**) with no observed cell viability at 80 μ M. In contrast with
396 resveratrol derivatives, alkylated catechins **18a** and **18b** displayed no toxicity, but association of
397 PUFA and alkyl on catechin backbone (**19a** and **19b**), resulted in high toxicity in the ARPE-19
398 cell line.

399



400

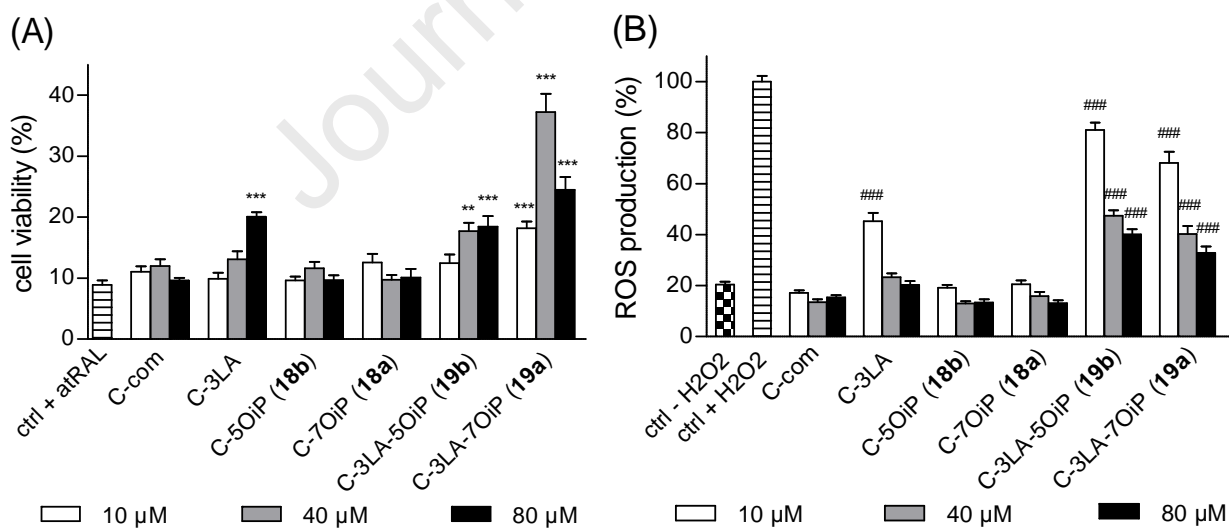
401 **Figure 6.** Evaluation of cytotoxicity of (+)-catechin derivatives; natural (+)-catechin (C-com), C-
 402 3LA [42], C-5OiP (**18b**), C-7OiP (**18a**), C-3LA-5OiP (**19b**) and C-3LA-7OiP (**19a**). Results are
 403 expressed in mean \pm SEM and are from n = 3-5 independent experiments. ARPE-19 cell viability
 404 (MTT) after incubation of catechin derivatives (0-160 μ M). The data are expressed as the
 405 percentage of non-treated control cells. * p < 0.05, ** p < 0.01, *** p < 0.001, versus non-
 406 treated control cells.

407

408 Interestingly, despite the absence of cell protection using C-com, C-3LA was able to display a
 409 mild protection against carbonyl stressor, with dose-dependent effects. The catechin ring, in
 410 contrast to resveratrol or phloroglucinol ring, should be nucleophilic enough to show a protective
 411 effect against carbonyl stressor, without the presence of isopropyl function on the resorcinol
 412 moiety (responsible for inductive effect). The direct trapping of RCS, such as methylglyoxal (an
 413 intermediate reactive carbonyl of AGE formation) by natural catechin was described in cell-free
 414 experiments by Peng et al. [56]. Wang confirmed this observation in 2010, by identifying
 415 adducts produced by co-incubation of catechin with glyoxal, methylglyoxal and acrolein [32].
 416 Zhu et al. also demonstrated trapping of lipid-derived α,β -unsaturated aldehydes, which have
 417 been implicated as causative agents in the development of carbonyl stress-associated pathologies
 418 (i.e. 4-HNE and acrolein), by several (poly)phenols including catechin [31]. However, most of

419 those adducts have been observed only under simulated physiological conditions but rarely in
 420 actual cellular media. As expected, in our work, the addition of isopropyl, preferentially at the 7
 421 position (C-3LA-7OiP (**19a**), **Figure 7A**), increased cellular protection when tested at 40 μ M
 422 (below the toxic concentration of **19a**). The position of the isopropyl group seemed to influence
 423 anti-carbonyl stress activity, as well as the cytotoxic profile of the derivatives. Alkylation at the 7
 424 position favor aldehyde trapping in both C8 and C6 positions, whereas alkylation at the 5
 425 position orients the formation of adduct only with C6. Both sites were reported in the literature to
 426 react with aldehyde, however, some work performed on the activity of epigallocatechin-3-*O*-
 427 gallate (EGCG) led only to the identification of the C8 adduct [57]. Unexpectedly, the most
 428 active lipophenol against carbonyl stress in this series, C-3LA-7OiP (**19a**), was also the most
 429 toxic compound.

430



431 **Figure 7.** *In vitro* anti-COS evaluation of (+)-catechin derivatives. Comparison of natural (+)-
 432 catechin (C-com), C-3LA [42], C-5OiP (**18b**), C-7OiP (**18a**), C-3LA-5OiP (**19b**) and C-3LA-
 433 7OiP (**19a**) activities. Results are expressed in mean \pm SEM and are from n = 3-5 independent

434 experiments. (A) Anti-carbonyl stress assay: ARPE-19 cell viability (MTT) after incubation of
435 catechin derivatives (0-80 μM) and *at*RAL (15 μM). The data are expressed as the percentage of
436 non-treated and non-exposed to *at*RAL control cells. * $p < 0.05$, ** $p < 0.01$, *** $p < 0.001$,
437 versus non-treated and exposed to *at*RAL cells. (B) Antioxidant assay: representation of ROS
438 production (DCFDA probe) after incubation of catechin derivatives (0-80 μM) and H_2O_2 (600
439 μM) in ARPE-19 cells. The data are expressed as the percentage of non-treated and exposed to
440 H_2O_2 cells. All conditions have a p -value < 0.001 versus non-treated and exposed to H_2O_2
441 control cells. # $p < 0.05$, ## $p < 0.01$, ### $p < 0.001$, versus non-treated and non-exposed to H_2O_2
442 cells.

443

444 As expected, C-com, and the two alkylated derivatives C-5OiP (**18b**) and C-7OiP (**18a**),
445 displayed the best antioxidant activity with equivalent ROS production levels compared to
446 control cells non-exposed to H_2O_2 , as shown in **Figure 7B**. With two substituents reducing free
447 phenolic functions, C-3LA-5OiP (**19b**) and C-3LA-7OiP (**19a**) displayed dose-dependent effects
448 on ROS produced by H_2O_2 treatment, with a decrease by up to 60% and 67% in ROS production,
449 respectively, at 80 μM .

450 Despite these interesting antioxidant properties, C-3LA-5OiP (**19b**) lacked potent anti-
451 carbonyl stress activity (only 10% increase in viability observed at 80 μM) and C-3LA-7OiP
452 (**19a**) showed high toxicity (no survival from 80 μM), making these derivatives less interesting
453 anti-COS candidates compared to the resveratrol series.

454

455 3.2. Quercetin lipophenols synthesis and evaluation

456 Lipophilic quercetins Q-3LA and Q-3DHA were produced as previously described [42] and
457 two original pathways were developed to access the lipophenol derivatives of quercetin-5OiP
458 (**29**) and quercetin-7OiP (**39a/b**) (**Scheme 4 and 5**).

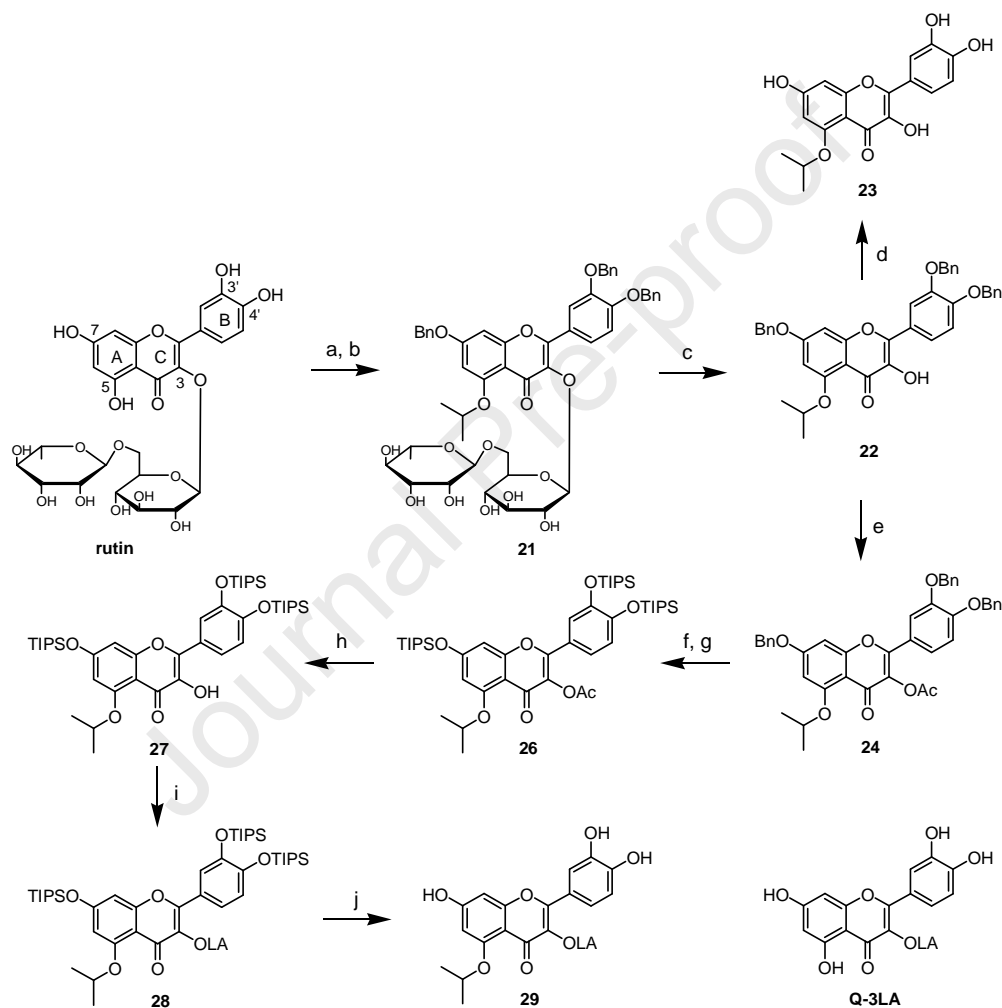
459

460 3.2.1. Quercetin-5OiP derivatives

461 A first chemical strategy was developed in order to access the liphenol derivative Q-3LA-
 462 5OiP (**29**) and the PUFA-free analogue Q-5OiP (**23**) (Scheme 4).

463

464 **Scheme 4. Synthesis and chemical structures of quercetin-5OiP derivatives^a**



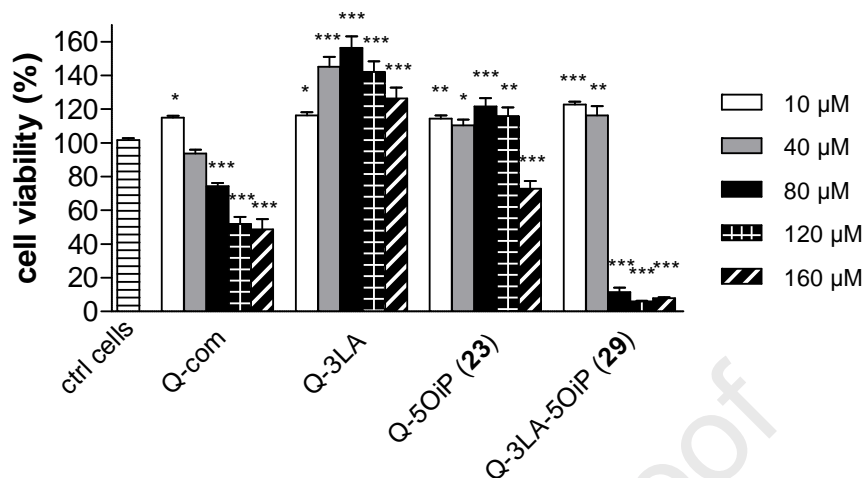
466 ^aReagents and conditions: (a) BnBr, K₂CO₃, DMF, 40 °C, 4 h, 61%; (b) 2-bromopropane,
 467 K₂CO₃, DMF, 80 °C, 18 h, 88%; (c) HCl, EtOH, 70 °C, 5 h, 98%; (d) H₂, Pd/C, THF/EtOH, rt,
 468 21 h, 69%; (e) pyridine, Ac₂O, rt, 20 h, 100%; (f) H₂, Pd/C, THF/EtOH, rt, 15 h, 100%; (g)
 469 TIPS-OTf, NEt₃, THF, rt, 4 h, 62%; (h) NH₃/MeOH, DCM, 0 °C, 3 h, 88%; (i) LA, DCC,
 470 DMAP, DCM, rt, 23 h, 54%; (j) NEt₃/3HF, THF, rt, 15 min, 72%.

471

472 In order to access quercetin-5OiP derivatives, we started from commercially available rutin
473 using the diholoside rutinoside as protecting group for the phenolic function at the 3 position.
474 The first step was the protection of the phenols in positions 7, 3' and 4' with benzyl groups.
475 Alkylation of the phenol in position 5 was performed with 2-bromopropane by heating at 80 °C
476 in dry DMF (88%). Cleavage of rutinoside in acidic conditions gave compound **22**, which was
477 either de-benzylated to access desired Q-5OiP (**23**), or acetylated in position 3 to pursue the
478 lipophenol synthesis. Benzyl groups were removed by hydrogenation to be replaced by silyl
479 protecting groups, which can be easily deprotected without damaging PUFA moiety leading to
480 compound **26**. Acetate in position 3 was then cleaved using ammonia solution in MeOH at 0 °C
481 to allow esterification with fatty acid. Final deprotection of TIPS group gave the desired Q-3LA-
482 5OiP (**29**).

483 For comparison purposes, commercial quercetin (Q-com) and Q-3LA [42] properties were also
484 evaluated *in vitro*. Under the conditions tested, Q-com was found to be toxic for the ARPE-19
485 cell line from 80 µM (**Figure 8**). Introduction of the isopropyl moiety (Q-5OiP, **23**) reduced the
486 toxicity with mild mortality starting at 160 µM. A similar reduction was observed with PUFA
487 introduction, as Q-3LA displayed no toxicity up to 160 µM, and was found to increase cell
488 viability (156% cell viability at 80 µM). However, the alkyl-lipophenol derivative Q-3LA-5OiP
489 (**29**) was very toxic, with no survival at 80 µM.

490



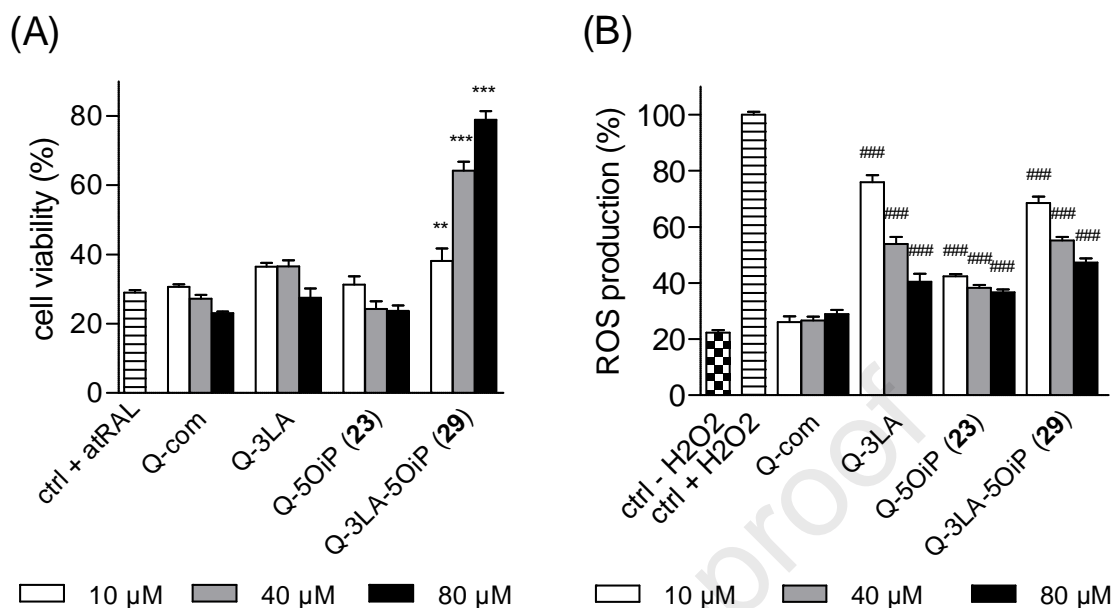
491

492 **Figure 8.** Evaluation of cytotoxicity of quercetin-5OiP derivatives; natural quercetin (Q-com),
 493 Q-3LA [42], Q-5OiP (**23**) and Q-3LA-5OiP (**29**). Results are expressed in mean \pm SEM and are
 494 from at $n = 3-5$ independent experiments. ARPE-19 cell viability (MTT) after incubation of
 495 quercetin-5OiP derivatives (0-160 μ M). The data are expressed as the percentage of non-treated
 496 control cells. * $p < 0.05$, ** $p < 0.01$, *** $p < 0.001$, versus non-treated control cells.

497

498 Regarding anti-carbonyl stress properties, here again the presence of isopropyl, as well as the
 499 PUFA moiety, seemed decisive for cell protection. As shown in **Figure 9A**, Q-com, Q-3LA and
 500 Q-5OiP (**23**) did not display any protective effect against *af*RAL toxicity, whereas Q-3LA-5OiP
 501 (**29**) protected cells with 50% increase in cell survival at 80 μ M. Even if toxic at 80 μ M, a high
 502 anti-carbonyl stress activity was observed at this concentration and can be explained by the
 503 differences between cytotoxicity and anti-carbonyl stress activity protocols (different incubation
 504 times).

505



506 **Figure 9.** *In vitro* anti-COS evaluation of quercetin-5OiP derivatives. Comparison of natural
 507 quercetin (Q-com), Q-3LA [42], Q-5OiP (**23**) and Q-3LA-5OiP (**29**) activities. Results are
 508 expressed as mean \pm SEM and are from $n = 3-5$ independent experiments. (A) Anti-carbonyl
 509 stress assay: ARPE-19 cell viability (MTT) after incubation of quercetin-5OiP derivatives (0-80
 510 μM) and arRAL (15 μM). The data are expressed as the percentage of non-treated and non-
 511 exposed to arRAL control cells. * $p < 0.05$, ** $p < 0.01$, *** $p < 0.001$, versus non-treated and
 512 exposed to arRAL cells. (B) Antioxidant assay: representation of ROS production (DCFDA
 513 probe) after incubation of quercetin-5OiP derivatives (0-80 μM) and H_2O_2 (600 μM) in ARPE-
 514 19 cells. The data are expressed as the percentage of non-treated and exposed to H_2O_2 cells. All
 515 conditions have a p -value < 0.001 versus non-treated and exposed to H_2O_2 control cells. # $p <$
 516 0.05, ## $p < 0.01$, ### $p < 0.001$, versus non-treated and non-exposed to H_2O_2 cells.

517

518 Finally, antioxidant capacity was evaluated and is reported in **Figure 9B**. The Di-substituted
 519 lipophenol derivative Q-3LA-5OiP (**29**) was efficient to reduce H_2O_2 -induced ROS production
 520 by 53% at 80 μM . Here again, a dose-dependent antioxidant potency was still observable despite
 521 the reduction of two free phenolic functions of quercetin. A similar protection profile was
 522 observed for the isopropyl-free analogue Q-3LA, which suggests that position 5 is not primordial
 523 for ROS scavenging activity. This was also confirmed by comparing Q-com and Q-5OiP (**23**)
 524 cell treatment, which led to low ROS levels.

525

526 To conclude, *in vitro* assessments indicate that in this series, alkylated resorcinol and PUFA
527 moieties are necessary for anti-carbonyl stress activity, as observed for the phloroglucinol [23]
528 and resveratrol series. Derivative Q-3LA-5OiP (**29**) displays interesting anti-COS properties,
529 however, its high cytotoxicity on ARPE-19 has to be considered for further evaluations.

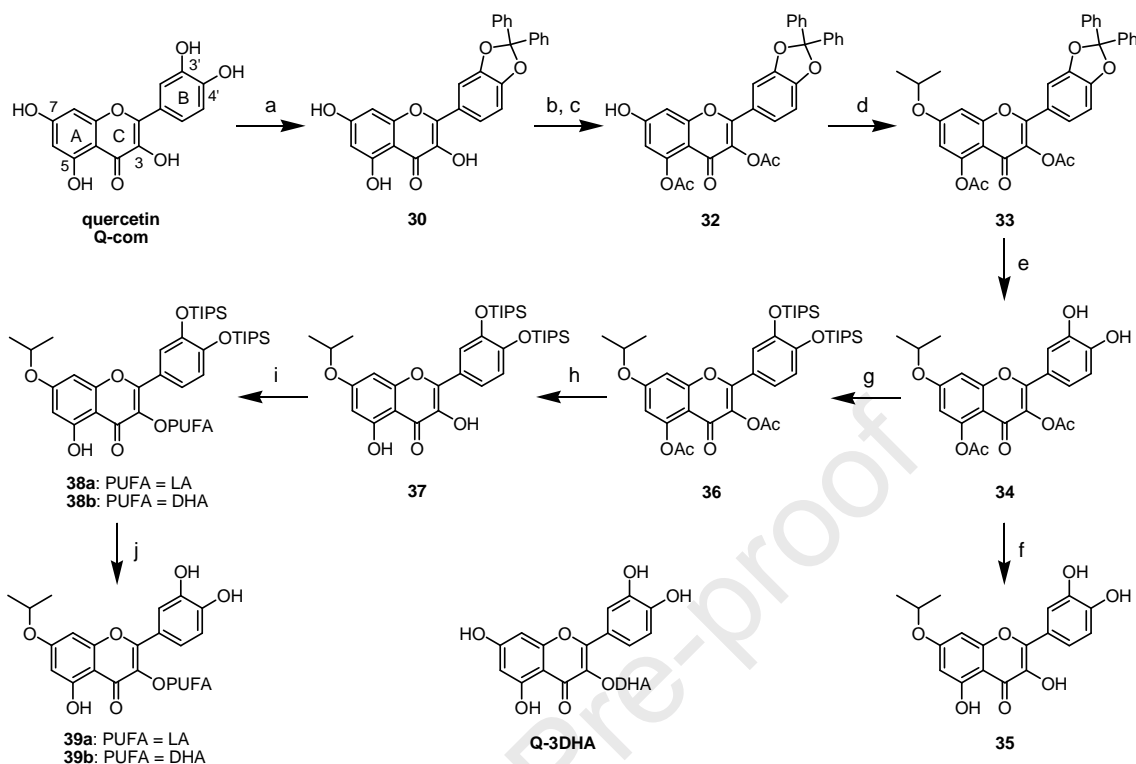
530

531 3.2.2. Quercetin-7OiP derivatives

532 A second chemical strategy, presented in **Scheme 5**, was developed for the synthesis of alkyl
533 quercetin Q-7OiP (**35**) and the two lipophenol derivatives Q-3LA-7OiP (**39a**) and Q-3DHA-
534 7OiP (**39b**).

535

536 **Scheme 5. Synthesis and chemical structures of quercetin-7OiP derivatives^a**



537

538 "Reagents and conditions: (a) Ph_2CCl_2 , Ph_2O , 175 °C, 2 h, 89%; (b) pyridine, Ac_2O , rt, 20 h,
 539 100%; (c) PhSH , imidazole, NMP, 0 to 5 °C, 5 h, 100%; (d) diisopropylsulfate, K_2CO_3 , acetone,
 540 rt, 22 h, 91%; (e) H_2 , $\text{Pd}(\text{OH})_2$, THF/EtOH, rt, 20 h, 47%; (f) NH_3/MeOH , 0 °C, 35 min, 46%;
 541 (g) TIPS-OTf, NEt_3 , THF, rt, 10 min, 71%; (h) NH_3/MeOH , DCM, 0 °C, 1 h, 100%; (i) PUFA,
 542 DCC, DMAP, DCM, rt, 5 h, **38a**: 86% and **38b**: 85%; (j) $\text{NEt}_3/3\text{HF}$, THF, rt, 30 min, 92% for
 543 **39a** and **39b**.

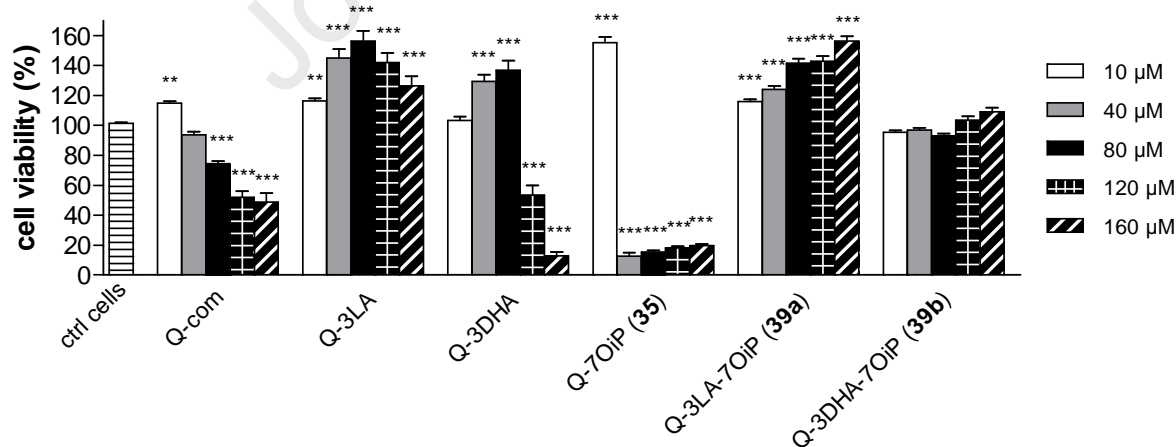
544

545 For the synthesis of Q-7OiP derivatives, the catechol of the commercial quercetin was first
 546 protected by diphenyldioxole, followed by the protection of the remaining phenolic functions
 547 with acetate moieties. Selective deprotection of phenol in position 7 was then performed
 548 according to Li et al., using thiophenol and imidazole in *N*-methylmorpholine in quantitative
 549 yield [58]. Compound **32** was then alkylated with diisopropylsulfate leading to derivative **33** in
 550 91% yield. Hydrogenation of diphenyldioxole with palladium hydroxide led to compound **34**,
 551 which can be either deacetylated to access desired Q-7OiP (**35**) or protected with silyl ethers to
 552 access protected derivative **36**. Deacetylation of **36** with diluted ammonia solution in MeOH at

553 0°C allowed access to compound **37**, which could be selectively esterified in position 3 by PUFA
 554 (86% for LA and 85% for DHA derivatives). Resulting compounds underwent a final TIPS
 555 deprotection leading to the desired lipophenol derivatives Q-3LA-7OiP (**39a**) and Q-3DHA-7OiP
 556 (**39b**).

557 Toxicity and activity of quercetin-7OiP lipophenols Q-3LA-7OiP (**39a**) and Q-3DHA-7OiP
 558 (**39b**), were compared to Q-com, Q-3LA [42], Q-3DHA [42] and Q-7OiP (**35**). Toxicity profile
 559 (**Figure 10**) shows that Q-7OiP (**35**) was highly toxic even at low concentrations with no
 560 survival observed at 40 μ M. The position of the alkyl moiety appeared critical, as Q-5OiP (**23**,
 561 **Figure 8**) did not display such high toxicity. Reduction of Q-com toxicity was observed by
 562 introduction of the PUFA moieties, as Q-3DHA and Q-3LA increased ARPE-19 cells viability
 563 from 10 to 80 μ M until toxicity appeared. Alkyl-lipophenol derivatives Q-3LA-7OiP (**39a**) and
 564 Q-3DHA-7OiP (**39b**) did not display any toxicity up to 160 μ M, and Q-3LA-7OiP (**39a**) even
 565 increased cell survival at 160 μ M (156% cell viability).

566



567

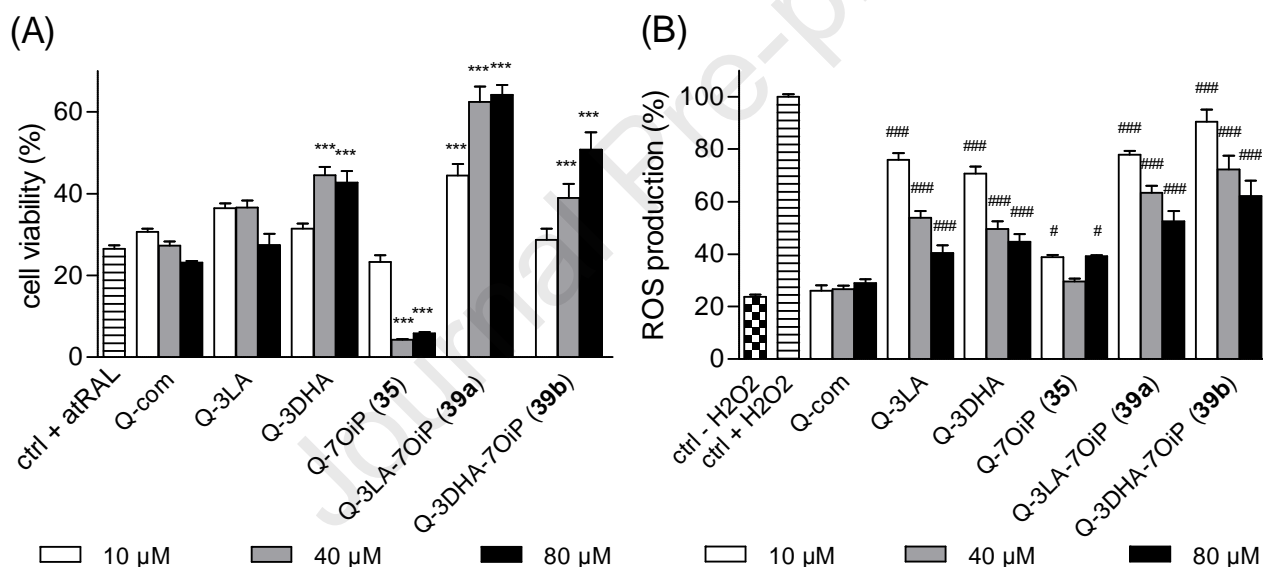
568 **Figure 10.** Evaluation of cytotoxicity of quercetin-7OiP derivatives; natural quercetin (Q-com),
 569 Q-3LA [42], Q-3DHA [42], Q-7OiP (**35**), Q-3LA-7OiP (**39a**) and Q-3DHA-7OiP (**39b**). Results
 570 are expressed in mean \pm SEM and are from n = 3-5 independent experiments. ARPE-19 cell

571 viability (MTT) after incubation of quercetin-7OiP derivatives (0-160 μ M). The data are
572 expressed as the percentage of non-treated control cells. * $p < 0.05$, ** $p < 0.01$, *** $p < 0.001$,
573 versus non-treated control cells.

574

575 As also observed for the resveratrol and catechin series, in our cellular assay the natural
576 quercetin alone did not protect against carbonyl stress toxicity (**Figure 11A**), whereas it has been
577 reported the formation of adduct by co-incubation of quercetin with several reactive aldehydes
578 (i.e. glyoxal, methylglyoxal and acrolein) in cell-free assays [32]. As expected regarding toxicity
579 profile, the PUFA-free quercetin Q-7OiP (**35**) is not protective against carbonyl stress and
580 presents high toxicity. Globally, the addition of the isopropyl on this lipophenol derivatives led
581 to an increase of cell protection against RCS, however, the impact of the isopropyl seemed less
582 important than in the resveratrol, phloroglucinol or quercetin-5OiP lipophenol series.
583 Comparison between the effect of Q-7OiP (**35**) and the alkyl-lipophenols Q-3LA-7OiP (**39a**) and
584 Q-3DHA-7OiP (**39b**) (increased viability by 38% and 24%, respectively, at 80 μ M) confirmed
585 the importance of the PUFA part to confer high cellular protection against *at*RAL toxicity using
586 alkyl-(poly)phenol (already observed in other series). Lipid peroxidation of PUFA produces
587 reactive aldehydes (4-HNE or 4-hydroxyhexenal (4-HHE)) [59]. Exposure to excessive 4-HNE
588 or 4-HHE can cause cytotoxicity and is implied in the detrimental pathogenesis of a number of
589 degenerative diseases [60]. However, such lipid peroxidation metabolites are also signaling
590 molecules able to induce gene expression of antioxidant and detoxifying aldehyde enzymes, by
591 activation of the Nrf2 pathway [61]. In ARPE-19, Johansson et al. reported the ability of DHA
592 treatment to induce cellular antioxidant responses, by Nrf2 pathway activation, and to stimulate
593 autophagy [62]. In addition, some works reported also the anti-glycation properties of PUFAs
594 [63,64]. As glycation reaction is caused by reactive aldehydes, anti-glycation properties can be
595 related to anti-carbonyl stress activity. Additional studies reported the cytoprotective effect of

596 PUFAs, by increasing S-phase cell promotion or lipid metabolism [65]. In the retina for example,
 597 DHA was shown to protect photoreceptors from oxidative stress by preserving mitochondrial
 598 membrane integrity [66]. In most of the (poly)phenol series studied in this work, the introduction
 599 of a PUFA part and an alkyl moiety on the (poly)phenol was a prerequisite to provide important
 600 cellular protection against *at*RAL toxicity. This may be due to improved cell penetration due to
 601 an increased lipophilicity, and/or a synergic effect of the alkyl-(poly)phenol and the PUFA
 602 moiety.
 603



604 **Figure 11.** *In vitro* anti-COS evaluation of quercetin-7OiP derivatives. Comparison of natural
 605 quercetin (Q-com), Q-3LA [42], Q-3DHA [42], Q-7OiP (35), Q-3LA-7OiP (39a) and Q-3DHA-
 606 7OiP (39b) activities. Results are expressed as mean \pm SEM and are from $n = 3-5$ independent
 607 experiments. (A) Anti-carbonyl stress assay: ARPE-19 cell viability (MTT) after incubation of
 608 quercetin-7OiP derivatives (0-80 μ M) and *at*RAL (15 μ M). The data are expressed as the
 609 percentage of non-treated and non-exposed to *at*RAL control cells. * $p < 0.05$, ** $p < 0.01$, *** p
 610 < 0.001 , versus non-treated and exposed to *at*RAL cells. (B) Antioxidant assay: representation of
 611 ROS production (DCFDA probe) after incubation of quercetin-7OiP derivatives (0-80 μ M) and
 612 H₂O₂ (600 μ M) in ARPE-19 cells. The data are expressed as the percentage of non-treated and
 613 exposed to H₂O₂ cells. All conditions have a p -value < 0.001 versus non-treated and exposed to

614 H₂O₂ control cells. # p < 0.05, ## p < 0.01, ### p < 0.001, versus non-treated and non-exposed to
615 H₂O₂ cells.

616

617 Antioxidant capacities of the derivatives are reported in **Figure 11B**. As expected, lower
618 antioxidant profile of the two lipophenols Q-3LA-7OiP (**39a**) and Q-3DHA-7OiP (**39b**),
619 compared to natural quercetin, can be explained by introduction of two substituents on phenolic
620 positions. However, Q-3LA-7OiP (**39a**) and Q-3DHA-7OiP (**39b**) displayed interesting dose-
621 dependent reduction of ROS close to the alkyl-free lipophenols Q-3DHA and Q-3LA. They
622 decreased by up to 48% and 38% of H₂O₂ induced ROS production, respectively, when
623 introduced at 80 μM.

624 The two di-substituted candidates Q-3LA-7OiP (**39a**) and Q-3DHA-7OiP (**39b**) are potent
625 anti-COS derivatives for further evaluations, as they displayed interesting dose-dependent
626 protection on ARPE-19 cell line and induced no toxicity up to 160 μM.

627

628 4. Selection of best anti-COS candidates in ARPE-19 cells

629 After systematic evaluation of our lipophenol derivatives, only the most promising candidates
630 were selected for further *in vitro* evaluations. Catechin and quercetin-5OiP lipophenols have
631 been rejected as they display important cytotoxicity in the ARPE-19 cell line. Regarding the
632 close protection provided by either LA or DHA lipophenols, omega-3 DHA lipophenols were
633 selected in view of *in vivo* evaluation. Indeed, many beneficial effects of DHA have been
634 reported in relation to retinal affections [67], such as anti-inflammatory, neuroprotective effects
635 [28,68] and antioxidant properties [66]. Visual processing deficits have been improved with
636 DHA supplementation in some clinical studies [25,67]. Moreover, as predominant PUFA of the
637 photoreceptor membrane, DHA is transported by several specific pathways across the Blood

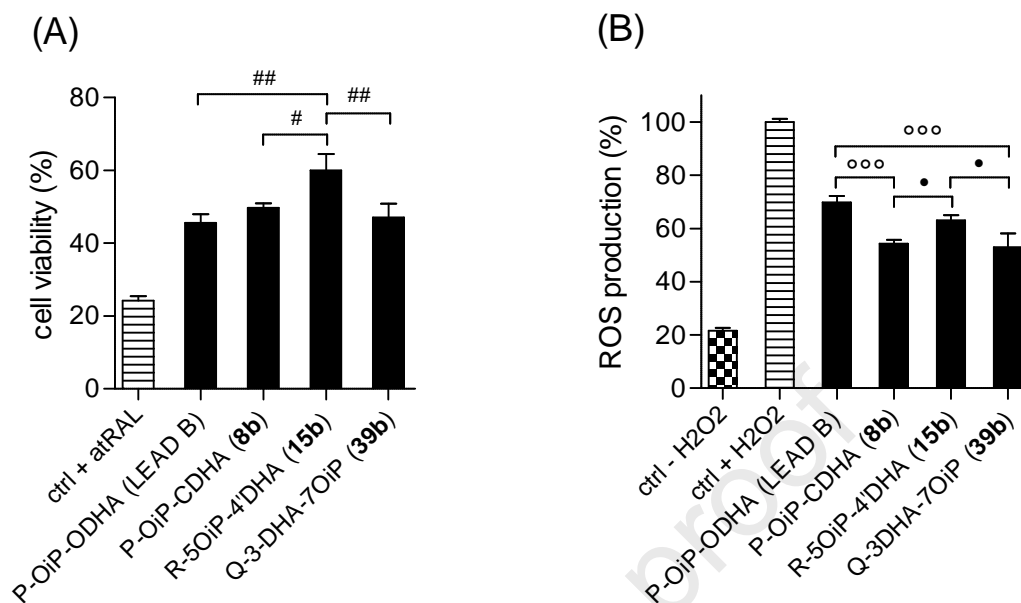
638 Retina Barrier (BRB) [69]. These properties of DHA are favorable, as increasing the lipophilicity
639 of (poly)phenols using this PUFA, can help the derivatives through retinal cell membranes and
640 across the RPE barrier. In order to select the best candidate for pharmacological development,
641 we compared anti-COS profiles of the most promising lipophenols. According to SAR study of
642 anti-COS assays, selected derivatives bear an isopropyl moiety, as well as DHA lipophilic
643 function.

644

645 *4.1. Anti-COS comparative assays*

646 All anti-COS activities of promising alkyl-DHA lipophenols have been summarized at the
647 same concentration (80 μ M) that displayed the best protective effects, and are represented in
648 **Figure 12**. The range of anti-carbonyl stress activity is similar for three of the four derivatives:
649 R-5OiP-4'DHA (**15b**) is the only compound that displayed a significantly higher protective
650 effect against *af*RAL toxicity compared to P-OiP-ODHA (LEAD B), P-OiP-CDHA (**8b**) or Q-
651 3DHA-7OiP (**39b**), as shown in **Figure 12A**.

652



653 **Figure 12.** Comparison of anti-COS activities of selected DHA alkyl-lipophenols: P-OiP-ODHA
 654 (LEAD B) [23], P-OiP-CDHA (**8b**), R-5OiP-4'DHA (**15b**) and Q-3DHA-7OiP (**39b**). Results
 655 are expressed as mean \pm SEM and are from $n = 3-5$ independent experiments. (A) Anti-carbonyl
 656 stress assay: ARPE-19 cell viability (MTT) after incubation of lipophenol derivatives (80 μ M)
 657 and *at*RAL (15 μ M). The data are expressed as the percentage of non-treated and non-exposed to
 658 *at*RAL control cells. All conditions have a p -value < 0.001 versus non-treated and exposed to
 659 *at*RAL control cells. # $p < 0.05$, ## $p < 0.01$, ### $p < 0.001$, versus R-5OiP-4'DHA (**15b**). (B)
 660 Antioxidant assay: representation of ROS production (DCFDA probe) after incubation of
 661 lipophenol derivatives (80 μ M) and H₂O₂ (600 μ M) in ARPE-19 cells. The data are expressed as
 662 the percentage of non-treated and exposed to H₂O₂ cells. All conditions have a p -value < 0.001
 663 versus non-treated and exposed to H₂O₂ control cells and versus non-treated and non-exposed to
 664 H₂O₂ control cells. ° $p < 0.05$, °° $p < 0.01$, °°° $p < 0.001$, versus P-OiP-ODHA (LEAD B). • $p <$
 665 0.05, •• $p < 0.01$, ••• $p < 0.001$, versus R-5OiP-4'DHA (**15b**).

666

667 The main objective of the (poly)phenol backbone modification was to overcome the low
 668 antioxidant activity of P-OiP-ODHA (LEAD B). This goal was achieved, as two of the three new
 669 lipophenol derivatives displayed a significant better efficiency against H₂O₂-induced ROS
 670 production when compared to the LEAD B: 16 and 17% reduction in ROS production for P-OiP-
 671 CDHA (**8b**) and Q-3DHA-7OiP (**39b**), respectively, as shown in **Figure 12B**. No significant
 672 difference in antioxidant evaluation was observed between P-OiP-ODHA (LEAD B) and R-

673 5OiP-4'DHA (**15b**). Lower efficacy of P-OiP-ODHA (LEAD B) and R-5OiP-4'DHA (**15b**)
674 could be explained by comparing their number of free phenolic positions as those lipophenols
675 only have one free phenolic function to scavenge ROS. Papuc et al. detailed structure-activity
676 relationship of (poly)phenol antioxidant activity and highlighted that not only the number of free
677 phenols is important for radical scavenging activity but also their position [70]. Indeed,
678 flavonoids with a catechol moiety (B-ring) are the most effective radical scavengers due to the
679 degree of stability conferred by the catechol structure participating in electron delocalization and
680 in the chelation of metals involved in ROS generation.

681

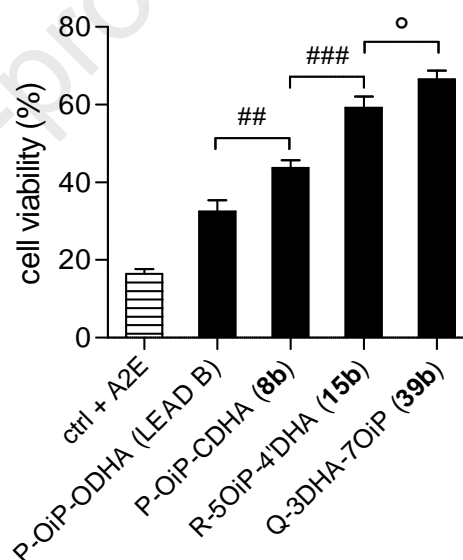
682 4.2. Protection against photo-induced A2E toxicity

683 Lipofuscin, a fluorescent lysosomal pigment composed of several lipophilic molecules (*bis*-
684 retinoids), is associated with age-related pathophysiological processes in the RPE. The best-
685 studied *bis*-retinoid and the first component of lipofuscin to be identified is A2E. Accumulation
686 and photo-oxidation of the di-retinal conjugate A2E in the RPE through ROS mechanisms are
687 known to be one of the critical causes of AMD [5–7,71]. Therefore, the reduction of lipid
688 oxidation is a promising approach to prevent the progression of AMD [72]. RPE cell death was
689 observed by photo-oxidation of A2E due to generation of singlet oxygen and superoxide radicals
690 [73]. A2E can be degraded in epoxide and aldehyde derivatives leading also to carbonyl stress
691 [7,74]. This is why we did not only evaluate the protective effects against *ar*RAL toxicity and
692 ROS scavenging properties herein. For an in-depth lipophenol comparison, a more specific
693 cellular assay is the evaluation of the protective effects of DHA alkyl-lipophenols against photo-
694 oxidized A2E toxicity, which more closely resembles AMD cytotoxicity.

695 Evaluation of survival of the RPE cell line ARPE-19 after incubation of lipophenols with A2E
 696 and photo-oxidation by intensive blue light was performed. As represented in **Figure 13**, the best
 697 protective effect was obtained for Q-3DHA-7OiP (**39b**) which increased cell viability by 50% at
 698 80 μ M, whereas P-OiP-ODHA (LEAD B) and P-OiP-CDHA (**8b**) only improved survival by
 699 16% and 27%, respectively. R-5OiP-4'DHA (**15b**) was also an interesting candidate, as it
 700 increased cell viability by 43% at 80 μ M.

701

Compound	A2E EC ₅₀ (μ M)
P-OiP-ODHA (LEAD B)	144.60 \pm 28.1
P-OiP-CDHA (8b)	63.99 \pm 9.73
R-5OiP-4'DHA (15b)	44.87 \pm 6.07
Q-3DHA-7OiP (39b)	15.38 \pm 2.53



702 **Figure 13.** DHA-lipophenols protection against photo-oxidized A2E toxicity. Comparison of P-
 703 OiP-ODHA (LEAD B) [23], P-OiP-CDHA (**8b**), R-5OiP-4'DHA (**15b**) and Q-3DHA-7OiP
 704 (**39b**) protection. Results are expressed as mean \pm SEM and are from n = 3-5 independent
 705 experiments. ARPE-19 cell viability (MTT) after incubation of lipophenol derivatives (80 μ M)
 706 and toxic concentration of photo-oxidized A2E (20 μ M, blue light exposure 30 min). The data
 707 are expressed as the percentage of non-treated and non-exposed to A2E control cells. EC₅₀ are
 708 calculated for all lipophenols using dose responses curves (0-80 μ M) and GraphPad prism
 709 software. All conditions have a p-value < 0.001 versus non-treated and exposed to toxic photo-
 710 oxidized A2E control cells. # p < 0.05, ## p < 0.01, ### p < 0.001, versus P-OiP-CDHA (**8b**). ° p
 711 < 0.05, °° p < 0.01, °°° p < 0.001, versus R-5OiP-4'DHA (**15b**).

712

713 All DHA-lipophenols are able to protect cells against photo-oxidized A2E toxicity. In order to
714 better compare the four selected alkyl-lipophenols, dose-dependent responses from 10 μM to 80
715 μM were performed to calculate Efficiency Concentration 50 (EC_{50}), the concentration of
716 lipophenol needed to protect 50% of the cells from photo-oxidized A2E toxicity. P-OiP-ODHA
717 (LEAD B) was less potent than the other derivatives with an EC_{50} of 145 μM . This can be
718 explained by its lower ROS scavenging ability. P-OiP-CDHA (**8b**) was significantly more
719 protective than P-OiP-ODHA (LEAD B) with an EC_{50} of 64 μM . This result was in accordance
720 with the anti-COS study, as both lipophenols displayed the same anti-carbonyl stress activity but
721 P-OiP-CDHA (**8b**) was more efficient at scavenging ROS than its lead P-OiP-ODHA (LEAD B).
722 Surprisingly, R-5OiP-4'DHA (**15b**) was more potent than P-OiP-CDHA (**8b**), protecting up to
723 59% of cells exposed to photo-oxidized A2E at 80 μM ($\text{EC}_{50} = 45 \mu\text{M}$), although it was less
724 efficient at scavenging ROS generated by H_2O_2 in the first antioxidant evaluation. However,
725 anti-carbonyl stress activity (higher for R-5OiP-4'DHA (**15b**) than P-OiP-CDHA (**8b**)) likely
726 participated in the protection of cells against photo-oxidized A2E. The most efficient lipophenol
727 against A2E toxicity is Q-3DHA-7OiP (**39b**) with an EC_{50} of 15 μM only and a maximal
728 viability of 67% of cells at 80 μM . Indeed, this lipophenol, which displayed an equivalent anti-
729 carbonyl stress activity as the others, was the most efficient in scavenging ROS and was
730 therefore the most protective in the assays. Comparison of natural (poly)phenols (i.e.
731 phloroglucinol, resveratrol and quercetin) in the A2E assay showed that quercetin was itself
732 more protective than phloroglucinol and resveratrol against photo-induced toxicity of A2E (data
733 not shown).

734 Among the three *in vitro* cell assays performed in this study and the toxicity profile, Q-3DHA-
735 7OiP (**39b**) has proven to be the most promising anti-COS lipophenol and R-5OiP-4'DHA (**15b**)
736 an interesting fallback solution.

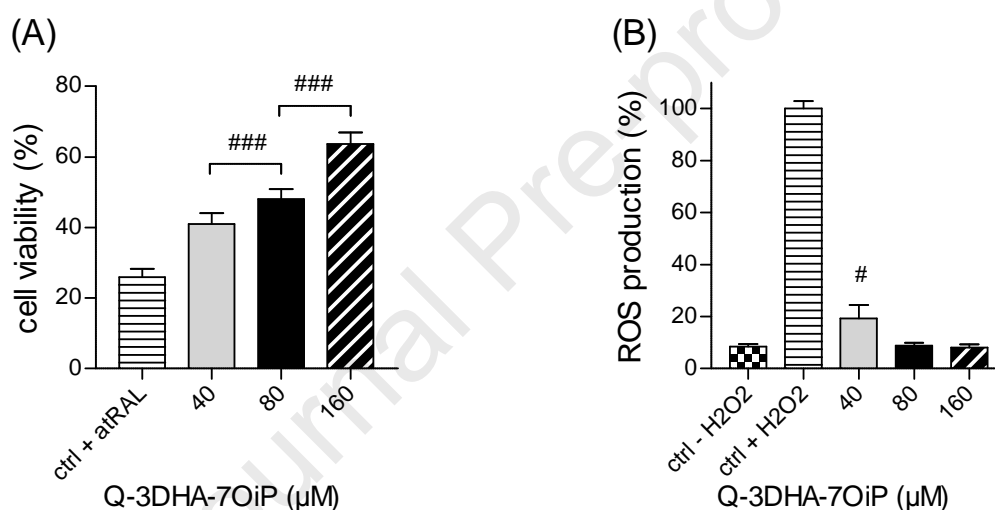
737

738 5. Validation of Q-3DHA-7OiP anti-COS properties in primary rat RPE cells

739 Currently, the ARPE-19 cell line and primary cultures are both sources of RPE cells for *in*
740 *vitro* models used in fundamental and applied research, including the development of new
741 approaches for ophthalmological disorders [75]. The advantage of cell lines is that they maintain
742 their characteristics over a number of passages and have longer survival times, compared to
743 primary cultures. Moreover, ARPE-19 can be plated at constant cell density throughout the
744 study, whereas primary cultures exhibit more cell density variability [24]. This cell density
745 depends on the cytotoxicity of *at*RAL and H₂O₂ [24,76]. Nevertheless, even if ARPE-19 cells are
746 a valuable model for human RPE cells, it seems important to validate the anti-COS effect of the
747 compounds on primary cells to be closer to the physiological protection *in vivo* [11]. However,
748 the production of primary RPE cells is tedious and time consuming work because it depends on
749 the number of eyeballs available [26,77]. Therefore, only the most promising lipophenol
750 derivative Q-3DHA-7OiP (**39b**) was evaluated in primary rat RPE cells for its protective action
751 against *at*RAL toxicity and ROS production. A dose-dependent increase in cell viability was
752 observed for cultures incubated with *at*RAL and Q-3DHA-7OiP (**39b**) and is represented in
753 **Figure 14A**. Treatment of primary RPE cells with *at*RAL (25 μ M) caused a significant decrease
754 in cell viability (26% of cell viability for untreated control cells), whereas treatment with *at*RAL
755 and Q-3DHA-7OiP (40, 80 and 160 μ M) significantly improved cell viability by 15%, 22% and
756 39%, respectively). Interestingly, the stress condition (25 μ M of *at*RAL), as well as treatment

757 with up to 80 μM Q-3DHA-7OiP, showed very similar effects in primary RPE and ARPE-19
 758 cells, suggesting that both stressor and protector use a common mechanism of action. By
 759 contrast, exposure of primary RPE cells to H_2O_2 at 600 μM for 4 h increased intracellular ROS
 760 levels by 12-fold compared to the untreated cells (Ctrl - H_2O_2). Moreover, cells treated with Q-
 761 3DHA-7OiP (40, 80 and 160 μM) markedly reduced ROS by 81%, 91% and 92%, respectively,
 762 in comparison to the non-treated cells, exposed to H_2O_2 (**Figure 14B**).

763



764 **Figure 14.** Anti-COS activity of Q-3DHA-7OiP (**39b**) on primary rat RPE cells. Results are
 765 expressed as mean \pm SEM and are from $n = 3$ -5 independent experiments. (A) Anti-carbonyl
 766 stress assay: cell viability (MTT) after incubation of Q-3DHA-7OiP (**39b**) (0-160 μM) and
 767 arRAL (25 μM). The data are expressed as the percentage of non-treated and non-exposed to
 768 arRAL control cells. All conditions have a p-value < 0.001 versus non-treated and exposed to
 769 arRAL control cells. # $p < 0.05$, ## $p < 0.01$, ### $p < 0.001$, versus 80 μM of lipophenol. (B)
 770 Antioxidant assay: representation of ROS production (DCFDA probe) after incubation of Q-
 771 3DHA-7OiP (**39b**) (0-160 μM) and H_2O_2 (600 μM) in primary cells. The data are expressed as
 772 the percentage of non-treated and exposed to H_2O_2 cells. All conditions have a p-value < 0.001
 773 versus non-treated and exposed to H_2O_2 control cells. # $p < 0.05$, ## $p < 0.01$, ### $p < 0.001$,
 774 versus non-treated and non-exposed to H_2O_2 cells.

775 The protective effects of Q-3DHA-7OiP (**39b**) on primary rat RPE cells fully validate the
 776 results obtained on ARPE-19 cells. This is particularly true with respect to the carbonyl stress

777 generated by *atRAL*, as the primary RPE showed a high protection effectiveness of Q-3DHA-
778 7OiP. This demonstrates the robustness of the results obtained on the cell line and suggests that
779 these data can be more easily extrapolated to *in vivo* assays. Moreover, Q-3DHA-7OiP (**39b**) is
780 now a lead for future investigations. The antioxidant activity is itself remarkable because it is
781 much more effective in the primary RPE compared to ARPE-19. Such a difference has already
782 been reported in the past with polyphenols, such as quercetin, especially in the context of
783 oxidative stress caused by H₂O₂ [76]. The authors reported that many of the flavonoids were
784 more effective at protecting primary RPE compared with ARPE-19. On this basis, it can be
785 speculated that quercetin derivative **39b** can protect retinal cell types through different
786 mechanisms, including direct scavenging of ROS, anti-apoptotic activity, and phase -2 induction
787 [78]. It was also shown that the most effective compounds are more hydrophobic than quercetin,
788 indicating that they should pass through cell membranes and accumulate intracellularly [79]. The
789 DHA combined with quercetin should be consistent with an increase in hydrophobicity and cell
790 bioavailability of the compound.

791

792 **Conclusions**

793 Among the research performed to develop pharmacological treatment for macular
794 degeneration, most of the molecules have been discarded in the past because of toxicity issues.
795 We propose here, a pharmacological approach based on a natural product ((poly)phenolic
796 compound linked to omega-3 derivatives). Both parts of the molecule have already proven their
797 beneficial effect in numerous studies as dietary complements: as (poly)phenols and omega-3
798 PUFAs are already present in our alimentation, the risk of toxicity compared to other synthetic

799 drugs may be considerably reduced, as well as the unwanted side effects. Naturally, *in vivo*
800 toxicity of lipophenols and their potential *α*RAL-adduct will have to be studied in future studies.

801 Starting from the phloroglucinol backbone, the present work evaluated the modification of the
802 (poly)phenol core to achieve protection against both carbonyl and oxidative stresses in RPE
803 cells. New synthetic routes were developed to access four original lipophenol series based on
804 phloroglucinol, resveratrol, catechin and quercetin (poly)phenols. Despite cell-free assays
805 proving aldehyde scavenging of natural (poly)phenols, our work highlights that, in biological
806 media, the protection against carbonyl stress (produced by *α*RAL toxicity) requires additional
807 chemical modifications of natural (poly)phenol to promote cellular protection. Both isopropyl-
808 resorcinol and PUFA moieties were essential for promising anti-carbonyl stress activity in RPE
809 cells. Substitution of two phenolic functions lower antioxidant capacity, compared to native
810 (poly)phenols, as reported in literature [22], however di-substituted alkyl-lipophenols still
811 provide sufficient antioxidant activities to reduce intracellular ROS. Despite significant literature
812 relating direct RCS trapping using (poly)phenols in cell-free assays, there is limited information
813 on this direct interaction in complex biological systems. This work highlights the importance of
814 cellular assays to validate anti-carbonyl stress potency of (poly)phenol conjugates: chemicals
815 able to scavenge aldehyde in cell-free assays are not necessarily active in biological media,
816 because of a lack of bioavailability or cell penetration, but also because of the importance of the
817 pH in RCS scavenging (increased in basic conditions) [80,81]. It is therefore relevant to consider
818 the pH dependency of the aldehyde trapping by (poly)phenol, as pH can vary from one cell
819 compartment to another. The exact mechanism of alkyl-lipophenol protection against *α*RAL
820 toxicity is currently under investigation and may be an association of 1) direct aldehyde
821 scavenging, chemically or enzymatically catalyzed [82]; 2) activation of aldehyde detoxification

822 enzymes, as the alkyl-phloroglucinol lipophenol LEAD B is able to activate Nrf2-Keap1
823 pathway [24] (also reported to activate aldehyde dehydrogenases and glutathione S-transferases
824 gene expression involved in aldehyde detoxification), and 3) reduction of ROS levels and
825 oxidative stress induced by *at*RAL cell treatment [24,26,83].

826 Taken together, the different cellular assays performed on the ARPE-19 cell line led to the
827 discovery of an optimal DHA-quercetin anti-COS lipophenol (Q-3DHA-7OiP, **39b**) showing
828 optimized antioxidant properties compared to the previous phloroglucinol lead (LEAD B), and
829 high protection against *at*RAL toxicity. Its anti-COS properties have also been validated in
830 primary RPE cells. To conclude, Q-3DHA-7OiP was the most powerful lipophenol to suppress
831 photo-oxidative toxicity initiated in RPE cells by A2E. Evaluation of photoreceptor protection
832 against acute light-induced degeneration in the *Abca4*^{-/-} mouse model (involving both carbonyl
833 and oxidative stresses), will be reported in due course using the best lipophenol candidate, Q-
834 3DHA-7OiP.

835

836 **Experimental Section**

837 **1. Chemical synthesis**

838 **Experimental Procedures.** The detailed discussion and the experimental procedures of
839 chemical/enzymatic synthesis of all intermediates and final lipophenols are described in the
840 supporting information (**sections S1 to S7**), as well as their full analytic characterization (¹H and
841 ¹³C NMR, HRMS analysis, R_f, melting point). Known compounds were prepared according to
842 previously described procedures: mono-isopropyl-phloroglucinol (**1**) and P-OiP-ODHA (LEAD
843 B) [23], P-OiP-OLA (LEAD A) [24], R-4'LA and R-4'DHA [43], Q-3LA, Q-3DHA and C-3LA
844 [42].

845

846 **2. Biological evaluations**

847 **Chemicals.** All lipophenols were dissolved in dimethylsulfoxide (DMSO) to prepare a stock
848 solution at 80 mM. Hydrogen peroxide solution (H₂O₂, 30 wt. % in H₂O), all-*trans* retinal
849 (*at*RAL) and 3-(4,5-dimethylthiazol-2-yl)-2,5-diphenyl tetrazolium bromide (MTT) were
850 purchased from Sigma-Aldrich. *N*-retinylidene-*N*-retinylethanolamine (A2E) was synthesized as
851 previously described by Parish et al. in 1998 [84]. 2',7'-dichlorofluorescein diacetate (DCFDA)
852 was purchased from Sigma-Aldrich (Saint-Quentin, France) and dissolved in DMSO to prepare
853 stock solution at 20 mM. All stock solutions of lipophenols, *at*RAL, A2E and probe were stored
854 at -20 °C in the dark.

855 **Cell Culture.** *ARPE-19* cells were obtained from ATCC (USA) and were grown in Dulbecco's
856 Modified Eagle's Medium (DMEM)/Ham F12 (GIBCO) containing 10% v/v fetal bovine serum
857 (FBS) and 1% v/v penicillin/streptomycin under atmospheric humidified air (95%) / CO₂ (5%) at
858 37 °C. For experimental cell seeding and sub-culturing, the cells were dissociated with 0.25%
859 trypsin-EDTA, resuspended in the culture medium and then plated at 1–3 × 10⁵ cells/mL. *ARPE-*
860 *19* cells were cultured and used up to 15 passages. *Primary RPE* cells were established from
861 Long-Evans newborn rats according to the procedure described previously [26,77]. Briefly, after
862 enucleation of the eyes, intact RPE sheets were separated from the choroid and dissociated in a
863 trypsin-EDTA solution (GIBCO) to obtain a suspension of single cells. RPE cells, cultured in 96-
864 well plates, reached 80–85% of confluence after 3 days in atmospheric humidified air (95%) /
865 CO₂ (5%) at 37 °C, and were used for cell assays without passaging.

866 **Cell Viability.** Cell viability was determined in *ARPE-19* and *primary rat RPE* cells by MTT
867 colorimetric assay. The cells were incubated for 2 h with MTT reagent (0.5 mg/mL). During this

868 incubation time, mitochondrial dehydrogenases of the living cells reduce the MTT to insoluble
869 purple formazan, which was then dissolved with DMSO to form a colored solution. The
870 absorbance of supernatants, which was proportional to the number of living cells, was measured
871 at 570 nm and 655 nm using a microplate reader (BioRad 550, USA or CLARIOstar Plus, BMG
872 Labtech). The absorbance of the compounds tested does not interfere with the absorbance at 570
873 and 655 nm. The percentage of the viable cells was calculated as $[(OD_{570} \text{ sample} - OD_{655} \text{ sample}) / (OD_{570} \text{ control} - OD_{655} \text{ control})] \times 100\%$.

875 **Cytotoxicity of Lipophenols.** ARPE-19 cells were plated into 96-well plates (4×10^4
876 cells/well) and cultured for 24 h to reach confluence before lipophenol treatment. The cell
877 cultures were treated with serum free medium containing the lipophenols at different
878 concentrations (0–160 μM) for 24 h. Control cells were incubated with DMSO (0.2%). The
879 viability of the cells was determined using MTT colorimetric assay, as described above, and
880 expressed as a percentage of viable cells normalized with control conditions in the absence of
881 lipophenols.

882 **Protection of Lipophenols against *at*RAL Toxicity.** ARPE-19 cells were plated into 96-well
883 plates (4×10^4 cells/well) and cultured for 24 h to reach confluence before lipophenol treatment.
884 The cell cultures were treated with serum free DMEM/F12 medium containing lipophenols at
885 different concentrations (0–80 μM) for 1 h. Then *at*RAL was added to a final concentration of 15
886 μM for 4 h before rinsing with medium. Control cells were incubated with DMSO (0.2%) \pm
887 *at*RAL. The cells incubated at 37 °C and viability was determined 16–20 h later using a MTT
888 colorimetric assay. For *primary rat RPE cultures*, cells were treated with *at*RAL (25 μM) in the
889 presence of lipophenol (40–160 μM) for 4 h before cell viability determination. Results are

890 expressed in percentage of viable cells normalized with control conditions in the absence of
891 lipophenol and stressor.

892 **Impact of Lipophenols on ROS Level.** ROS level was measured in *ARPE-19* and *primary rat*
893 *RPE cells* using dichlorofluorescein diacetate (DCFDA) reagent. The cell permeant reagent
894 DCFDA is deacetylated by cellular esterases to dichlorofluorescein (DCFH₂), which can be
895 oxidized by several radical reactive species (peroxyl, alkoxy, NO₂[•], carbonate, HO[•], ...) into the
896 fluorophore 2',7'-dichlorofluorescein (DCF) [85]. Intensity of fluorescence was measured
897 during DCFDA oxidation by radical species to calculate level of radical reactive species. *ARPE-*
898 *19 cells* were plated into black, optically clear flat bottom 96-well plates (4×10^4 cells/well) and
899 cultured for 24 h to reach confluence before the drug treatment. The cell cultures were incubated
900 with 2 μ M of DCFDA for 45 min in DMEM/F12 medium without phenol red + 1% FBS. The
901 cells were rinsed and incubated with the medium containing lipophenols at different
902 concentrations (0–80 μ M) for 1 h. Then, H₂O₂ was added to a final concentration of 600 μ M for
903 4 h. *Primary rat RPE cells* were seeded on white, opaque-bottomed 96-well plates. On day 3,
904 cells were incubated for 45 minutes at 37 °C in 1X Buffer containing 25 μ M of DCFDA. The
905 cells were then treated with 600 μ M of H₂O₂ in the presence of lipophenol (40–160 μ M) for 4 h
906 at 37 °C. For both *ARPE-19* and *primary cells*, DCF production was measured by fluorescence
907 spectroscopy with excitation wavelength at 485 nm and emission wavelength at 535 nm. The
908 fluorescence of the compounds tested does not interfere with DCFDA signal. Control cells were
909 incubated with DMSO (0.2%) \pm DCFDA \pm H₂O₂. The percentage of ROS produced was
910 calculated as [(fluorescence of sample)/(fluorescence of control)] \times 100%. The results are
911 expressed in percentage of ROS produced normalized with control conditions in the absence of
912 lipophenol and presence of H₂O₂.

913 **Protection of Lipophenols against Photo-Oxidized A2E Toxicity.** ARPE-19 cells were
914 plated into 96-well plates (4×10^4 cells/well) and cultured for 24 h to reach confluence before
915 lipophenol treatment. The cell cultures were treated with serum free DMEM/F12 medium
916 without phenol red containing lipophenols at different concentrations (0–80 μM) for 1 h. Then
917 A2E was added to a final concentration of 20 μM for 6 h before rinsing with medium. Control
918 cells were incubated with DMSO (0.2%) \pm A2E. The cells were exposed to intense blue light
919 (4600 LUX) for 30 min to induce phototoxicity of A2E and incubated at 37 °C. The cell viability
920 was determined 16–20 h later using a MTT colorimetric assay. Results are expressed as a
921 percentage of viable cells normalized with control conditions in the absence of lipophenols and
922 stressor. When a dose-dependent efficiency was observed, EC_{50} was calculated.

923 **Statistical Analysis.** The data are presented as means \pm SEM determined from at least three
924 independent experiments. In each experiment, all conditions were done at least in quadruplicate.
925 Statistical analyses were performed by Oneway ANOVA test using Newman-Keuls's post-hoc
926 for Gaussian distributions (the normality of distributions was evaluated with a Shapiro-Wilk test)
927 and differences with p-values < 0.05 were considered as statistically significant. EC_{50} were
928 calculated using GraphPad Prism version 5.03 and non-linear regression.

929

930 **Associated Content**

931 **Supporting Information**

932 Full discussion on chemical synthesis of C-phloroglucinol derivatives (**Section S1**);
933 Characterization of the silylated chromane orthoester byproduct of compound **5** (**Section S2**);
934 Full discussion on chemical synthesis of resveratrol derivatives (**Section S3**); Full discussion on
935 chemical synthesis of (+)-catechin derivatives (**Section S4**); Full discussion on chemical
936 synthesis of quercetin-5O_iP derivatives (**Section S5**); Full discussion on chemical synthesis of

937 quercetin-7O*i*P derivatives (**Section S6**); Experimental procedure and full analysis
938 characterization of all intermediates and final compounds (**2a** to **39b**, **Section S7**); ¹H and ¹³C
939 NMR spectra for all intermediates and final compounds (**2a** to **39b**, **Section S8**).

940

941 **Author Contributions**

942 All authors contributed to the writing of the manuscript. All authors gave approval to the final
943 version of the manuscript. PB and CC contributed equally to this work.

944 **Funding Sources**

945 This research was funded by University of Montpellier, SATT AxLR (181088BU) and ANR
946 (LipoPheRet - ANR-18-CE18-0017). Inserm and CNRS are thanked for their support.

947

948 **Acknowledgments**

949 The authors would like to thank Dr. Gaetan Drouin and Pr. Vincent Rioux for providing DHA-
950 ethyl ester necessary for lipophenol synthesis, and Dr. Vasiliki Kalatzis for English correction of
951 the manuscript.

952

953 **References**

954 [1] J.Z. Nowak, Oxidative stress, polyunsaturated fatty acids-derived oxidation products and
955 bisretinoids as potential inducers of CNS diseases: focus on age-related macular degeneration,
956 *Pharmacol. Rep.* 65 (2013) 288–304.

- 957 [2] J.R. Sparrow, E. Gregory-Roberts, K. Yamamoto, A. Blonska, S.K. Ghosh, K. Ueda, J.
958 Zhou, The Bisretinoids of Retinal Pigment Epithelium, *Prog. Retin. Eye Res.* 31 (2012) 121–
959 135.
- 960 [3] J.T. Handa, M. Cano, L. Wang, S. Datta, T. Liu, Lipids, oxidized lipids, oxidation-
961 specific epitopes, and Age-related Macular Degeneration, *Biochim. Biophys. Acta* 1862 (2017)
962 430–440.
- 963 [4] A.V. Cideciyan, T.S. Aleman, M. Swider, S.B. Schwartz, J.D. Steinberg, A.J. Brucker,
964 A.M. Maguire, J. Bennett, E.M. Stone, S.G. Jacobson, Mutations in ABCA4 result in
965 accumulation of lipofuscin before slowing of the retinoid cycle: a reappraisal of the human
966 disease sequence, *Hum Mol Genet.* 13 (2004) 525–534.
- 967 [5] J.R. Sparrow, N. Fishkin, J. Zhou, B. Cai, Y.P. Jang, S. Krane, Y. Itagaki, K. Nakanishi,
968 A2E, a byproduct of the visual cycle, *Vision Res.* 43 (2003) 2983–2990.
- 969 [6] S.R. Kim, S. Jockusch, Y. Itagaki, N.J. Turro, J.R. Sparrow, Mechanisms involved in
970 A2E oxidation, *Exp. Eye Res.* 86 (2008) 975–982.
- 971 [7] Y. Wu, E. Yanase, X. Feng, M.M. Siegel, J.R. Sparrow, Structural characterization of
972 bisretinoid A2E photocleavage products and implications for age-related macular degeneration,
973 *Proc. Natl. Acad. Sci. U. S. A.* 107 (2010) 7275–7280.
- 974 [8] A.E. Sears, P.S. Bernstein, A.V. Cideciyan, C. Hoyng, P.C. Issa, K. Palczewski, P.J.
975 Rosenfeld, S. Sadda, U. Schraermeyer, J.R. Sparrow, I. Washington, H.P.N. Scholl, Towards
976 Treatment of Stargardt Disease: Workshop Organized and Sponsored by the Foundation Fighting
977 Blindness, *Transl. Vis. Sci. Technol.* 6 (2017) 1–32.

- 978 [9] D. Kook, A.H. Wolf, A.L. Yu, A.S. Neubauer, S.G. Priglinger, A. Kampik, U.C. Welge-
979 Lussen, The protective effect of quercetin against oxidative stress in the human RPE in vitro,
980 *Invest Ophthalmol. Vis. Sci.* 49 (2008) 1712–1720.
- 981 [10] R.E. King, K.D. Kent, J.A. Bomser, Resveratrol reduces oxidation and proliferation of
982 human retinal pigment epithelial cells via extracellular signal-regulated kinase inhibition, *Chem.*
983 *Biol. Interact.* 151 (2005) 143–149.
- 984 [11] W. Kalt, A. Hanneken, P. Milbury, F. Tremblay, Recent research on polyphenolics in
985 vision and eye health, *J. Agric. Food Chem.* 58 (2010) 4001–4007.
- 986 [12] S. Quideau, D. Deffieux, C. Douat-Casassus, L. Pouységu, Plant Polyphenols: Chemical
987 Properties, Biological Activities, and Synthesis, *Angew. Chem. Int. Ed.* 50 (2011) 586–621.
- 988 [13] H.J. Forman, K.J.A. Davies, F. Ursini, How do nutritional antioxidants really work:
989 Nucleophilic tone and para-hormesis versus free radical scavenging in vivo, *Free Radic. Biol.*
990 *Med.* 66 (2014) 24–35.
- 991 [14] Y. Xie, X. Chen, Structures required of polyphenols for inhibiting advanced glycation
992 end products formation, *Curr. Drug Metab.* 14 (2013) 414–431.
- 993 [15] I. Sadowska-Bartosz, G. Bartosz, Prevention of Protein Glycation by Natural
994 Compounds, *Molecules.* 20 (2015) 3309–3334.
- 995 [16] C.Y. Lo, W.T. Hsiao, X.Y. Chen, Efficiency of trapping methylglyoxal by phenols and
996 phenolic acids, *J. Food Sci.* 76 (2011) 90–96.

- 997 [17] X. Shao, H. Chen, Y. Zhu, R. Sedighi, C.-T. Ho, S. Sang, Essential Structural
998 Requirements and Additive Effects for Flavonoids to Scavenge Methylglyoxal, *J. Agric. Food*
999 *Chem.* 62 (2014) 3202–3210.
- 1000 [18] W. Wang, Y. Qi, J.R. Rocca, P.J. Sarnoski, A. Jia, L. Gu, Scavenging of Toxic Acrolein
1001 by Resveratrol and Hesperetin and Identification of Adducts, *J. Agric. Food Chem.* 63 (2015)
1002 9488–9495.
- 1003 [19] F. Yin, X. Wang, Y. Hu, H. Xie, X. Liu, L. Qin, J. Zhang, D. Zhou, F. Shahidi,
1004 Evaluation of Absorption and Plasma Pharmacokinetics of Tyrosol Acyl Esters in Rats, *J. Agric.*
1005 *Food Chem.* 68 (2020) 1248–1256.
- 1006 [20] O.M. Feeney, M.F. Crum, C.L. McEvoy, N.L. Trevaskis, H.D. Williams, C.W. Pouton,
1007 W.N. Charman, C.A.S. Bergström, C.J.H. Porter, 50 years of oral lipid-based formulations:
1008 Provenance, progress and future perspectives, *Adv. Drug Deliv. Rev.* 101 (2016) 167–194.
- 1009 [21] C.W. Pouton, Lipid formulations for oral administration of drugs: non-emulsifying, self-
1010 emulsifying and ‘self-microemulsifying’ drug delivery systems, *Eur. J. Pharm. Sci.* 11 (2000)
1011 S93–S98.
- 1012 [22] C. Crauste, M. Rosell, T. Durand, J. Vercauteren, Omega-3 polyunsaturated lipophenols,
1013 how and why?, *Biochimie.* 120 (2016) 62–74.
- 1014 [23] C. Crauste, C. Vigor, P. Brabet, M. Picq, M. Lagarde, C. Hamel, T. Durand, J.
1015 Vercauteren, Synthesis and Evaluation of Polyunsaturated Fatty Acid–Phenol Conjugates as
1016 Anti-Carbonyl-Stress Lipophenols, *Eur. J. Org. Chem.* (2014) 4548–4561.

- 1017 [24] A. Cubizolle, D. Cia, E. Moine, N. Jacquemot, L. Guillou, M. Rosell, C. Angebault
1018 Prouteau, G. Lenaers, I. Meunier, J. Vercauteren, T. Durand, C. Crauste, P. Brabet, Isopropyl-
1019 phloroglucinol-DHA protects outer retinal cells against lethal dose of all-trans-retinal, *J. Cell.*
1020 *Mol. Med.* 24 (2020) 5057–5069.
- 1021 [25] T. Georgiou, A. Neokleous, D. Nicolaou, B. Sears, Pilot study for treating dry age-related
1022 macular degeneration (AMD) with high-dose omega-3 fatty acids, *PharmaNutrition.* 2 (2014) 8–
1023 11.
- 1024 [26] D. Cia, A. Cubizolle, C. Crauste, N. Jacquemot, L. Guillou, C. Vigor, C. Angebault, C.P.
1025 Hamel, J. Vercauteren, P. Brabet, Phloroglucinol protects retinal pigment epithelium and
1026 photoreceptor against all-trans-retinal-induced toxicity and inhibits A2E formation, *J. Cell.*
1027 *Mol. Med.* 20 (2016) 1651–1663.
- 1028 [27] M. Suh, A.A. Wierzbicki, E. Lien, M.T. Clandinin, Relationship between dietary supply
1029 of long-chain fatty acids and membrane composition of long- and very long chain essential fatty
1030 acids in developing rat photoreceptors, *Lipids.* 31 (1996) 61–64.
- 1031 [28] P.K. Mukherjee, V.L. Marcheselli, C.N. Serhan, N.G. Bazan, Neuroprotectin D1: a
1032 docosahexaenoic acid-derived docosatriene protects human retinal pigment epithelial cells from
1033 oxidative stress, *Proc. Natl. Acad. Sci. U. S. A.* 101 (2004) 8491–8496.
- 1034 [29] P. Brabet, A. Cubizolle, C. Crauste, L. Guillou, A.L. Bonnefont, J. Vercauteren, T.
1035 Durand, C.P. Hamel, A phloroglucinol-DHA derivative protects against light-induced retinal
1036 degeneration in an Abca4-deficient mouse model, *Invest. Ophthalmol. Vis. Sci.* 58 (2017) 2031.

- 1037 [30] N. Taveau, A. Cubizolle, L. Guillou, N. Piquier, E. Moine, D. Cia, J. Vercauteren, T.
1038 Durand, C. Crauste, P. Brabet, Preclinical pharmacology of a lipophenol in a mouse model of
1039 light-induced retinopathies., *Exp. Mol. Med.* 52 (2020) 1090–1101.
- 1040 [31] Q. Zhu, Z.-P. Zheng, K.-W. Cheng, J.-J. Wu, S. Zhang, Y.S. Tang, K.-H. Sze, J. Chen, F.
1041 Chen, M. Wang, Natural polyphenols as direct trapping agents of lipid peroxidation-derived
1042 acrolein and 4-hydroxy-trans-2-nonenal, *Chem. Res. Toxicol.* 22 (2009) 1721–1727.
- 1043 [32] W. Wang, Antiglycation effects and reactive carbonyl trapping capacity of berry and
1044 grape phytochemicals, Thesis of master of sciences of University of Florida. (2010) 1–129.
- 1045 [33] A. Alaimo, M.C. Di Santo, A.P. Domínguez Rubio, G. Chaufan, G. García Liñares, O.E.
1046 Pérez, Toxic effects of A2E in human ARPE-19 cells were prevented by resveratrol: a potential
1047 nutritional bioactive for age-related macular degeneration treatment, *Arch. Toxicol.* 94 (2020)
1048 553–572.
- 1049 [34] Y. Wang, H.J. Kim, J.R. Sparrow, Quercetin and cyanidin-3-glucoside protect against
1050 photooxidation and photodegradation of A2E in retinal pigment epithelial cells, *Exp. Eye Res.*
1051 160 (2017) 45–55.
- 1052 [35] W. Li, Y. Jiang, T. Sun, X. Yao, X. Sun, Supplementation of procyanidins B2 attenuates
1053 photooxidation-induced apoptosis in ARPE-19 cells, *Int. J. Food Sci. Nutr.* 67 (2016) 650–659.
- 1054 [36] O. Gia, A. Anselmo, M.T. Conconi, C. Antonello, E. Uriarte, S. Caffieri, 4'-Methyl
1055 Derivatives of 5-MOP and 5-MOA: Synthesis, Photoreactivity, and Photobiological Activity, *J.*
1056 *Med. Chem.* 39 (1996) 4489–4496.

- 1057 [37] M.J. So, E.J. Cho, Phloroglucinol Attenuates Free Radical-induced Oxidative Stress,
1058 *Prev. Nutr. Food Sci.* 19 (2014) 129–135.
- 1059 [38] M. Vestergaard, H. Ingmer, Antibacterial and antifungal properties of resveratrol, *Int. J.*
1060 *Antimicrob. Agents.* 53 (2019) 716–723.
- 1061 [39] J.-H. Kang, S.-Y. Choung, Protective effects of resveratrol and its analogs on age-related
1062 macular degeneration in vitro, *Arch. Pharm. Res.* 39 (2016) 1703–1715.
- 1063 [40] A. Lançon, R. Frazzi, N. Latruffe, Anti-Oxidant, Anti-Inflammatory and Anti-
1064 Angiogenic Properties of Resveratrol in Ocular Diseases, *Molecules.* 21 (2016) 1–8.
- 1065 [41] I.C. Vlachogianni, E. Fragopoulou, I.K. Kostakis, S. Antonopoulou, In vitro assessment
1066 of antioxidant activity of tyrosol, resveratrol and their acetylated derivatives, *Food Chem.* 177
1067 (2015) 165–173.
- 1068 [42] E. Moine, P. Brabet, L. Guillou, T. Durand, J. Vercauteren, C. Crauste, New Lipophenol
1069 Antioxidants Reduce Oxidative Damage in Retina Pigment Epithelial Cells, *Antioxidants.* 7
1070 (2018) 1–18.
- 1071 [43] A. Shamseddin, C. Crauste, E. Durand, P. Villeneuve, G. Dubois, T. Pavlickova, T.
1072 Durand, J. Vercauteren, F. Veas, Resveratrol-Linoleate protects from exacerbated endothelial
1073 permeability via a drastic inhibition of the MMP-9 activity, *Biosci. Rep.* (2018) 1–13.
- 1074 [44] C. Cren-Olivé, S. Lebrun, C. Rolando, An efficient synthesis of the four mono
1075 methylated isomers of (+)-catechin including the major metabolites and of some dimethylated
1076 and trimethylated analogues through selective protection of the catechol ring, *J. Chem. Soc.*
1077 *Perkin 1.* (2002) 821–830.

- 1078 [45] Y. Shen, Z. Xu, Z. Sheng, Ability of resveratrol to inhibit advanced glycation end product
1079 formation and carbohydrate-hydrolyzing enzyme activity, and to conjugate methylglyoxal, Food
1080 Chem. 216 (2017) 153–160.
- 1081 [46] S.-J. Sheu, N.-C. Liu, C.-C. Ou, Y.-S. Bee, S.-C. Chen, H.-C. Lin, J.Y.H. Chan,
1082 Resveratrol Stimulates Mitochondrial Bioenergetics to Protect Retinal Pigment Epithelial Cells
1083 From Oxidative Damage, Invest. Ophthalmol. Vis. Sci. 54 (2013) 6426–6438.
- 1084 [47] K.E. Heim, A.R. Tagliaferro, D.J. Bobilya, Flavonoid antioxidants: chemistry,
1085 metabolism and structure-activity relationships, J. Nutr. Biochem. 13 (2002) 572–584.
- 1086 [48] S.D.S. Banjarnahor, N. Artanti, Antioxidant properties of flavonoids, Med. J. Indones. 23
1087 (2015) 239–244.
- 1088 [49] R. Khursheed, S.K. Singh, S. Wadhwa, M. Gulati, A. Awasthi, Enhancing the potential
1089 preclinical and clinical benefits of quercetin through novel drug delivery systems, Drug Discov.
1090 Today. 25 (2020) 209-222.
- 1091 [50] H. Kalantari, H. Foruozandeh, M.J. Khodayar, A. Siahpoosh, N. Saki, P. Kheradmand,
1092 Antioxidant and hepatoprotective effects of Capparis spinosa L. fractions and Quercetin on tert-
1093 butyl hydroperoxide- induced acute liver damage in mice, J. Tradit. Complement. Med. 8 (2018)
1094 120–127.
- 1095 [51] A.J. Dugas, J. Castañeda-Acosta, G.C. Bonin, K.L. Price, N.H. Fischer, G.W. Winston,
1096 Evaluation of the Total Peroxyl Radical-Scavenging Capacity of Flavonoids: Structure–Activity
1097 Relationships, J. Nat. Prod. 63 (2000) 327–331.

- 1098 [52] K.L. Wolfe, R.H. Liu, Structure–Activity Relationships of Flavonoids in the Cellular
1099 Antioxidant Activity Assay, *J. Agric. Food Chem.* 56 (2008) 8404–8411.
- 1100 [53] S. Hong, S. Liu, Targeted acylation for all the hydroxyls of (+)-catechin and evaluation of
1101 their individual contribution to radical scavenging activity, *Food Chem.* 197 (2016) 415–421.
- 1102 [54] N.I. Howard, M.V.B. Dias, F. Peyrot, L. Chen, M.F. Schmidt, T.L. Blundell, C. Abell,
1103 Design and Structural Analysis of Aromatic Inhibitors of Type II Dehydroquinase from
1104 *Mycobacterium tuberculosis*, *ChemMedChem.* 10 (2015) 116–133.
- 1105 [55] S. Uesato, K. Taniuchi, A. Kumagai, Y. Nagaoka, R. Seto, Y. Hara, H. Tokuda, H.
1106 Nishino, Inhibitory effects of 3-O-acyl-(+)-catechins on Epstein-Barr virus activation, *Chem.*
1107 *Pharm. Bull.* 51 (2003) 1448–1450.
- 1108 [56] X. Peng, K.-W. Cheng, J. Ma, B. Chen, C.-T. Ho, C. Lo, F. Chen, M. Wang, Cinnamon
1109 Bark Proanthocyanidins as Reactive Carbonyl Scavengers To Prevent the Formation of
1110 Advanced Glycation Endproducts, *J. Agric. Food Chem.* 56 (2008) 1907–1911.
- 1111 [57] C.-Y. Lo, S. Li, D. Tan, M.-H. Pan, S. Sang, C.-T. Ho, Trapping reactions of reactive
1112 carbonyl species with tea polyphenols in simulated physiological conditions, *Mol. Nutr. Food*
1113 *Res.* 50 (2006) 1118–1128.
- 1114 [58] M. Li, X. Han, B. Yu, Facile Synthesis of Flavonoid 7- *O* -Glycosides, *J. Org. Chem.* 68
1115 (2003) 6842–6845.
- 1116 [59] B. Yang, R. Li, T. Woo, J.D. Browning, H. Song, Z. Gu, J. Cui, J.C. Lee, K.L. Fritsche,
1117 D.Q. Beversdorf, G.Y. Sun, C.M. Greenlief, Maternal Dietary Docosahexaenoic Acid Alters

- 1118 Lipid Peroxidation Products and (n-3)/(n-6) Fatty Acid Balance in Offspring Mice, *Metabolites*.
1119 9 (2019) 1–14.
- 1120 [60] Y. Huang, W. Li, A.-N.T. Kong, Anti-oxidative stress regulator NF-E2-related factor 2
1121 mediates the adaptive induction of antioxidant and detoxifying enzymes by lipid peroxidation
1122 metabolite 4-hydroxynonenal, *Cell Biosci.* 2 (2012) 1–7.
- 1123 [61] A. Ishikado, K. Morino, Y. Nishio, F. Nakagawa, A. Mukose, Y. Sono, N. Yoshioka, K.
1124 Kondo, O. Sekine, T. Yoshizaki, S. Ugi, T. Uzu, H. Kawai, T. Makino, T. Okamura, M.
1125 Yamamoto, A. Kashiwagi, H. Maegawa, 4-Hydroxy hexenal derived from docosaehaenoic acid
1126 protects endothelial cells via Nrf2 activation, *PLoS One.* 8 (2013) 1–13.
- 1127 [62] I. Johansson, V.T. Monsen, K. Pettersen, J. Mildenerger, K. Misund, K. Kaarniranta, S.
1128 Schønberg, G. Bjørkøy, The marine n-3 PUFA DHA evokes cytoprotection against oxidative
1129 stress and protein misfolding by inducing autophagy and NFE2L2 in human retinal pigment
1130 epithelial cells, *Autophagy.* 11 (2015) 1636–1651.
- 1131 [63] Z. Sun, X. Peng, J. Liu, K.-W. Fan, M. Wang, F. Chen, Inhibitory effects of microalgal
1132 extracts on the formation of advanced glycation endproducts (AGEs), *Food Chem.* 120 (2010)
1133 261–267.
- 1134 [64] M. Odjakova, E. Popova, M.A. Sharif, R. Mironova, Plant-Derived Agents with Anti-
1135 Glycation Activity, in: S. Petrescu (Eds.), *Glycosylation*, IntechOpen Publishing, chapter
1136 10,2012: pp. 223-256.

- 1137 [65] S.A. Belal, A.S. Sivakumar, D.R. Kang, S. Cho, H.S. Choe, K.S. Shim, Modulatory
1138 effect of linoleic and oleic acid on cell proliferation and lipid metabolism gene expressions in
1139 primary bovine satellite cells, *Anim. Cells Syst.* 22 (2018) 324–333.
- 1140 [66] N.P. Rotstein, L.E. Politi, O.L. German, R. Girotti, Protective Effect of Docosahexaenoic
1141 Acid on Oxidative Stress-Induced Apoptosis of Retina Photoreceptors, *Invest. Ophthalmol. Vis.*
1142 *Sci.* 44 (2003) 2252–2259.
- 1143 [67] J.P. SanGiovanni, E.Y. Chew, The role of omega-3 long-chain polyunsaturated fatty
1144 acids in health and disease of the retina, *Prog. Retin. Eye Res.* 24 (2005) 87–138.
- 1145 [68] E.E. Martínez Leo, R.A. Rojas Herrera, M.R. Segura Campos, Protective Effect of
1146 Omega 3 Fatty Acids EPA and DHA in the Neurodegenerative Disease, in: J.-M. Mérillon, K.G.
1147 Ramawat (Eds.), *Bioact. Mol. Food*, Springer International Publishing, Cham, 2018: pp. 1–17.
- 1148 [69] M. Tachikawa, S. Akanuma, T. Imai, S. Okayasu, T. Tomohiro, Y. Hatanaka, K. Hosoya,
1149 Multiple Cellular Transport and Binding Processes of Unesterified Docosahexaenoic Acid in
1150 Outer Blood–Retinal Barrier Retinal Pigment Epithelial Cells, *Biol. Pharm. Bull.* 41 (2018)
1151 1384–1392.
- 1152 [70] C. Papuc, G.V. Goran, C.N. Predescu, V. Nicorescu, G. Stefan, Plant Polyphenols as
1153 Antioxidant and Antibacterial Agents for Shelf-Life Extension of Meat and Meat Products:
1154 Classification, Structures, Sources, and Action Mechanisms, *Compr. Rev. Food Sci. Food Saf.*
1155 16 (2017) 1243–1268.

- 1156 [71] J.R. Sparrow, H.R. Vollmer-Snarr, J. Zhou, Y.P. Jang, S. Jockusch, Y. Itagaki, K.
1157 Nakanishi, A2E-epoxides Damage DNA in Retinal Pigment Epithelial Cells, *J. Biol. Chem.* 278
1158 (2003) 18207–18213.
- 1159 [72] M. Wrona, M. Rózanowska, T. Sarna, Zeaxanthin in combination with ascorbic acid or α -
1160 tocopherol protects ARPE-19 cells against photosensitized peroxidation of lipids, *Free Radic.*
1161 *Biol. Med.* 36 (2004) 1094–1101.
- 1162 [73] V.M. Parmar, T. Parmar, E. Arai, L. Perusek, A. Maeda, A2E-associated cell death and
1163 inflammation in retinal pigmented epithelial cells from human induced pluripotent stem cells,
1164 *Stem Cell Res.* 27 (2018) 95–104.
- 1165 [74] S. Ben-Shabat, Y. Itagaki, S. Jockusch, J.R. Sparrow, N.J. Turro, K. Nakanishi,
1166 Formation of a Nonaoxirane from A2E, a Lipofuscin Fluorophore related to Macular
1167 Degeneration, and Evidence of Singlet Oxygen Involvement, *Angew. Chem. Int. Ed.* 41 (2002)
1168 814–817.
- 1169 [75] A.V. Kuznetsova, A.M. Kurinov, M.A. Aleksandrova, Cell Models to Study Regulation
1170 of Cell Transformation in Pathologies of Retinal Pigment Epithelium, *J. Ophthalmol.* (2014) 1–
1171 18.
- 1172 [76] A. Hanneken, F.-F. Lin, J. Johnson, P. Maher, Flavonoids Protect Human Retinal
1173 Pigment Epithelial Cells from Oxidative-Stress-Induced Death, *Invest. Ophthalmol. Vis. Sci.* 47
1174 (2006) 3164–3177.

- 1175 [77] D. Cia, J. Vergnaud-Gauduchon, N. Jacquemot, M. Doly, Epigallocatechin Gallate
1176 (EGCG) Prevents H₂O₂-Induced Oxidative Stress in Primary Rat Retinal Pigment Epithelial
1177 Cells, *Curr. Eye Res.* 39 (2014) 944–952.
- 1178 [78] E. Pawlowska, J. Szczepanska, A. Koskela, K. Kaarniranta, J. Blasiak, Dietary
1179 Polyphenols in Age-Related Macular Degeneration: Protection against Oxidative Stress and
1180 Beyond, *Oxid. Med. Cell. Longev.* 2019 (2019) 1–13.
- 1181 [79] K. Ishige, D. Schubert, Y. Sagara, Flavonoids protect neuronal cells from oxidative stress
1182 by three distinct mechanisms, *Free Radic. Biol. Med.* 30 (2001) 433–446.
- 1183 [80] H. Zhu, M.M. Poojary, M.L. Andersen, M.N. Lund, Effect of pH on the reaction between
1184 naringenin and methylglyoxal: A kinetic study, *Food Chem.* 298 (2019) 1–9.
- 1185 [81] S. Sang, X. Shao, N. Bai, C.-Y. Lo, C.S. Yang, C.-T. Ho, Tea Polyphenol (–)-
1186 Epigallocatechin-3-Gallate: A New Trapping Agent of Reactive Dicarbonyl Species, *Chem. Res.*
1187 *Toxicol.* 20 (2007) 1862–1870.
- 1188 [82] B. Szwergold, Reactions between methylglyoxal and its scavengers in-vivo appear to be
1189 catalyzed enzymatically, *Med. Hypotheses.* 109 (2017) 153–155.
- 1190 [83] Y. Chen, K. Okano, T. Maeda, V. Chauhan, M. Golczak, A. Maeda, K. Palczewski,
1191 Mechanism of All- *trans* -retinal Toxicity with Implications for Stargardt Disease and Age-
1192 related Macular Degeneration, *J. Biol. Chem.* 287 (2012) 5059–5069.
- 1193 [84] C.A. Parish, M. Hashimoto, K. Nakanishi, J. Dillon, J. Sparrow, Isolation and one-step
1194 preparation of A2E and iso-A2E, fluorophores from human retinal pigment epithelium, *Proc.*
1195 *Natl. Acad. Sci. U. S. A.* 95 (1998) 14609–14613.

1196 [85] B. Halliwell, M. Whiteman, Measuring reactive species and oxidative damage in vivo
1197 and in cell culture: how should you do it and what do the results mean?, Br. J. Pharmacol. 142
1198 (2004) 231–255.

1199

Journal Pre-proof

Highlights

- Carbonyl and oxidative stresses play a crucial role in macular degeneration.
- All-*trans*-retinal accumulates abnormally in AMD causing toxic A2E formation.
- Lipophenol derivatives are polyphenols functionalized with PUFA.
- Quercetin lipophenol is a potent photo-oxidative toxicity suppressor in RPE cells.
- Lipophenols protect against toxicity induced by carbonyl and oxidative stresses.